





ORIGINAL ARTICLE

Morphofunctional characterization of hemocytes in black soldier fly larvae

Daniele Bruno^{1,*}, Aurora Montali^{1,*}, Marzia Gariboldi¹, Anna Katarzyna Wrońska² ,
Agata Kaczmarek², Amr Mohamed³ , Ling Tian⁴ , Morena Casartelli^{5,6}
and Gianluca Tettamanti^{1,6} 

¹Department of Biotechnology and Life Sciences, University of Insubria, Varese, Italy; ²Host Parasites Molecular Interaction Research Unit, Witold Stefański Institute of Parasitology, Polish Academy of Sciences, Warsaw, Poland; ³Department of Entomology, Faculty of Science, Cairo University, Giza, Egypt; ⁴Guangdong Provincial Key Laboratory of Agro-animal Genomics and Molecular Breeding, Guangdong Provincial Sericulture and Mulberry Engineering Research Center, College of Animal Science, South China Agricultural University, Guangzhou, China; ⁵Department of Biosciences, University of Milano, Milano, Italy and ⁶Interuniversity Center for Studies on Bioinspired Agro-environmental Technology (BAT Center), University of Napoli Federico II, Portici, Italy

Abstract In insects, the cell-mediated immune response involves an active role of hemocytes in phagocytosis, nodulation, and encapsulation. Although these processes have been well documented in multiple species belonging to different insect orders, information concerning the immune response, particularly the hemocyte types and their specific function in the black soldier fly *Hermetia illucens*, is still limited. This is a serious gap in knowledge given the high economic relevance of *H. illucens* larvae in waste management strategies and considering that the saprophagous feeding habits of this dipteran species have likely shaped its immune system to efficiently respond to infections. The present study represents the first detailed characterization of black soldier fly hemocytes and provides new insights into the cell-mediated immune response of this insect. In particular, in addition to prohemocytes, we identified five hemocyte types that mount the immune response in the larva, and analyzed their behavior, role, and morphofunctional changes in response to bacterial infection and injection of chromatographic beads. Our results demonstrate that the circulating phagocytes in black soldier fly larvae are plasmatocytes. These cells also take part in nodulation and encapsulation with granulocytes and lamellocyte-like cells, developing a starting core for nodule/capsule formation to remove/encapsulate large bacterial aggregates/pathogens from the hemolymph, respectively. These processes are supported by the release of melanin precursors from crystal cells and likely by mobilizing nutrient reserves in newly circulating adipohemocytes, which could thus trophically support other hemocytes during the immune response. Finally, the regulation of the cell-mediated immune response by eicosanoids was investigated.

Key words eicosanoids; encapsulation; hemocytes; *Hermetia illucens*; immunity; phagocytosis

Correspondence: Gianluca Tettamanti, Department of Biotechnology and Life Sciences, University of Insubria, Via J. H. Dunant, 3–21100 Varese, Italy. Email: gianluca.tettamanti@uninsubria.it

*Daniele Bruno and Aurora Montali contributed equally to the work.

Introduction

In insects, cellular and humoral components of the immune system are rapidly triggered by different non-self agents to counteract infections (Eleftherianos *et al.*, 2021a). Although the distinction between cellular and

humoral immune reactions as two different categories is not straightforward, hemocytes represent key players in almost all the processes by which insects clear foreign agents from their body. In fact, these circulating cells are not only directly involved in the mechanisms underlying the cellular response, such as phagocytosis, nodulation, and encapsulation (Strand, 2008; Eleftherianos *et al.*, 2021a); they are largely responsible for producing most of the humoral components, too. For example, intermediates of the prophenoloxidase (proPO) cascade, lysozyme, and antimicrobial peptides are synthesized by both the fat body and hemocytes (Lemaître & Hoffmann, 2007; Eleftherianos *et al.*, 2021b).

Considerable effort has been invested in studying and classifying hemocyte populations in Diptera (Lanot *et al.*, 2001; Pal & Kumar, 2014), Lepidoptera (Tan *et al.*, 2013; Boguś *et al.*, 2018), Coleoptera (Kwon *et al.*, 2014), Orthoptera (Cho & Cho, 2019), Hemiptera (Schmitz *et al.*, 2012), and Hymenoptera (Gábor *et al.*, 2020). In these studies, multiple types of hemocytes were identified, each with a specific role, and significant differences were demonstrated not only among insect orders, but also among genera that belong to the same order (Hillyer & Christensen, 2002; Nakahara *et al.*, 2009; Gábor *et al.*, 2020). This complex scenario is mostly the result of the multitude of morphological, histochemical, and molecular markers that have been used to study these immune cells over the years (Eleftherianos *et al.*, 2021a). Hence, the nomenclature and terminology used to designate hemocytes vary among insect species and differ from order to order and species to species. For example, while granulocytes, plasmacytes, spherulocytes, and oenocytoids are the cells most widely described in Lepidoptera (Nakahara *et al.*, 2009), plasmacytes, crystal cells, and lamellocytes, but not granulocytes, were reported in the dipteran *Drosophila melanogaster* (Brehélin, 1982). A comparison with other Diptera, such as *Aedes aegypti* and *Culex quinquefasciatus*, which share the presence of oenocytoids, and *Glossina morsitans*, in which they are absent (Kaaya & Ratcliffe, 1982), clearly demonstrates that species of this order do not share a general hemocyte pattern. A further level of complexity arises if we consider that different hemocyte types can perform the same function in different insect orders, such as for crystal cells of *D. melanogaster* and oenocytoids of Lepidoptera, which both produce proPO (Ribeiro & Brehélin, 2006).

The rapid activation of hemocytes by different nonself agents (Hillyer *et al.*, 2003a; Manachini *et al.*, 2011) promotes proliferation and activation of phagocytosis and/or encapsulation processes that last for a long time (Hillyer *et al.*, 2003a; Ling & Yu, 2006; Hwang *et al.*, 2015), indicating that the cellular component of the

immune system is maintained active until the threat is completely brought under control. However, as mentioned above, hemocytes also intervene in the production of several humoral molecules. Larvae of the dipteran *Hermetia illucens* infected with bacteria represent an interesting example, where 3 h are sufficient to start transcription of antimicrobial peptide-coding genes in hemocytes, whereas remarkable transcription levels can be detected only later (6–14 h) in the fat body (Bruno *et al.*, 2021), confirming the key role of hemocytes to quickly counteract bacterial cell proliferation.

In insects, the rapid and coordinated activation of cellular and humoral processes is mediated by the diffusion of various signaling molecules produced upon bacterial challenge (Kim *et al.*, 2018). Among them, eicosanoids act as ultimate downstream mediators in many physiological processes in insects, including activation of the cellular immune response (Stanley, 2006; Stanley & Kim, 2014). Eicosanoids are oxidized derivatives of 20-carbon polyunsaturated fatty acids, most frequently arachidonic acid (C20:4n-6) metabolites (Kim *et al.*, 2018). They include prostaglandins, thromboxanes, leukotrienes, and lipoxins biosynthesized by enzymatic oxygenation reactions of these fatty acids. In insects, hemocytes and the fat body produce eicosanoids, frequently through the hydrolysis of phospholipids by phospholipase A2 (PLA2). These metabolites are fundamental in activating cell-mediated processes such as phagocytosis, nodulation, and encapsulation in different insect orders (Stanley, 2006; Stanley & Kim, 2014).

Due to the marked differences in hemocyte pattern and behavior, it is mandatory to expand our knowledge of immune cells in insects and investigate how they respond to different immune challenges, especially in those species that are increasingly being used for their relevant economic importance (Cappelozza *et al.*, 2019; Tettamanti *et al.*, 2022). In this respect, the larvae of the black soldier fly (BSF), *H. illucens*, are attracting growing interest as they can be reared on different organic waste and the insect biomass can then become a valuable source of protein and lipids for feed formulation (Hawkey *et al.*, 2021), bioplastic manufacturing (Nuvoli *et al.*, 2021), and biodiesel production (Jung *et al.*, 2022). The ability of these larvae to grow on decaying materials, which are potentially rich in pathogens, has likely contributed to shape their immune system to efficiently respond to infections. However, studies of the immune response of this insect are limited (Vogel *et al.*, 2018; Bruno *et al.*, 2021; Vogel *et al.*, 2022) and very little is known about the morphological and functional features of its hemocytes (Zdybicka-Barabas *et al.*, 2017; von Bredow *et al.*, 2021).

To expand knowledge on the immune response of BSF larvae, herein we assessed if (i) certain hemocyte types are key players in specific cellular responses; (ii) the percentage and dynamics of hemocyte population change in response to infection; and (iii) eicosanoids mediate cellular immune interactions. To evaluate these aspects, we performed an in-depth characterization of hemocytes in *H. illucens* larvae and explored the roles they play in response to immune challenge; we also examined the involvement of eicosanoids in the modulation of hemocyte populations in response to immune challenge.

Materials and methods

Insect rearing

Insects were reared according to Pimentel *et al.* (2017). Briefly, after hatching, larvae were placed in a humid chamber and fed on standard diet for Diptera (50% wheat bran, 30% corn meal, and 20% alfalfa meal mixed at a 1 : 1 ratio dry matter : water) (Hogsette, 1992). After 4 days, batches of 300 larvae were placed in 16 × 16 × 9-cm plastic containers with ventilated lid, fed on the same diet, and kept in the dark at 27 ± 0.5 °C and 70% ± .5% relative humidity. Once at the pupal stage, insects were removed from the rearing substrate and transferred to a net cage until adult eclosion. Flies were maintained at 30 ± 0.5 °C, 70% ± 5% relative humidity, with a 12 : 12 h light : dark photoperiod and reared as brood stock (Bruno *et al.*, 2019a).

Bacterial strains and chromatographic beads

Escherichia coli (Strain K12, Merck, Darmstadt, Germany) and *Micrococcus luteus* ATCC No. 4698 (Merck) were selected for challenging the larvae with bacteria (Bruno *et al.*, 2021). After growing bacteria in 10 mL of Luria–Bertani medium (Merck) overnight at 37 °C under shaking at 160 r/min, 1-mL aliquots of both cultures were centrifuged at 1620 × *g* for 15 min. Cell pellets were washed with phosphate buffer (38 mmol/L KH₂PO₄, 61.4 mmol/L K₂HPO₄, pH 7.4) and then centrifuged at 1620 × *g* for 15 min. The optical density of bacterial cultures was measured at 600 nm (one unit of OD_{600nm} corresponds to 4.12 × 10⁸ colony-forming units [CFU]/mL of *E. coli* and 1.83 × 10⁷ CFU/mL of *M. luteus*) and bacterial stocks at 2 × 10⁵ CFU/mL were prepared by resuspending cell pellets in phosphate-buffered saline (PBS, 137 mmol/L NaCl, 2.7 mmol/L KCl, 10 mmol/L Na₂HPO₄/KH₂PO₄, pH 7.4). An *E. coli*/*M. luteus* mix at a concentration of 1 × 10⁵ CFU/mL was used for infect-

ing the larvae (each larva was injected with 5 μL of the bacterial mix) (Bruno *et al.*, 2021).

B-Agarose and DEAE-Sephadex A-25 beads (Merck) were selected for analyzing encapsulation (Bruno *et al.*, 2021). Before injection into the larvae, beads were washed and resuspended in sterile PBS, approximately 5 beads/μL.

Injection of larvae and hemolymph collection

Last instar larvae were washed with tap water to remove the rearing substrate from the cuticle and then with 0.5% sodium hypochlorite (in tap water, volume/volume [v/v]) and 70% ethanol (in distilled water, v/v). Insects were injected with: (i) 5 μL of 1 × 10⁵ CFU/mL *E. coli*/*M. luteus* mix with a Hamilton 700 10-μL syringe (Hamilton, Reno, NV, USA) or (ii) 5 μL of B-Agarose or DEAE-Sephadex A-25 beads (Merck) with a sterile 1-mL disposable syringe. Injections were performed between the third last and penultimate metamere of the larva. To avoid infections caused by bacteria present in the diet, injected larvae were kept under sterile conditions at 27 ± 0.5 °C and 70% ± .5% relative humidity, in the absence of feeding substrate. As the aim of the present study was to analyze the cell-mediated response triggered by the entrance of bacteria through lesions on the body surface, uninjected larvae (naïve) were used as controls, as reported previously (Bruno *et al.*, 2021). To exclude unwanted side effects caused by needle puncturing or PBS injection, specific control experiments were conceived. In detail, total hemocyte count, as well as quantification of adipohemocytes, crystal cells, and granulocytes, were performed by using the hemolymph collected from larvae subjected to puncture with a sterile needle or injected with 5 μL of sterile PBS. Results confirmed a significant difference between control groups and infected larvae (Supporting Information Fig. S1).

Larvae were analyzed from 5 min to 24 h after injection of bacteria or beads (see Results for details). They were rapidly cooled down on ice for 30 s and the hemolymph was collected by cutting the cephalic region with sterile scissors and gently squeezing the larva. The number of hemocytes collected from these larvae was compared with that from larvae kept at room temperature to exclude that the exposure of insects to low temperatures for a few seconds could affect the amount of immune cells (1590 ± 80 hemocytes/μL at low temperature and 1567 ± 53 hemocytes/μL at room temperature—the experiments were performed in triplicate).

The hemolymph was collected in plastic tubes on ice to avoid proPO activation. About 20 μL of hemolymph

was collected from each larva. Each experiment was performed in triplicate by pooling samples of hemolymph collected from at least 15 larvae; for transmission electron microscopy (TEM), flow cytometry, quantification of prostaglandin E₂ (PGE₂), and analysis of PLA2 activity, hemolymph was collected from at least 50 larvae.

Hemocyte characterization and quantification

Hemocyte counts After collection, hemolymph was diluted 1 : 10 with 0.4% Trypan blue (ThermoFisher, Waltham, MA, USA) and loaded into FAST READ 102 counting chambers (Biosigma S.R.L., Cona, Italy). The total number of hemocytes in control larvae and larvae injected with bacteria was calculated according to the manufacturer's instructions.

Giemsa staining and differential hemocyte counts A 200- μ L sample of hemolymph was poured on sterile round glass coverslips, kept in the dark for 15 min to allow the adhesion of hemocytes to the glass, and then cells were fixed with 5% formalin in PBS. Coverslips were air-dried and incubated for 10 min using the MGG quick stain kit (Bio-Optica, Milano, Italy) (diluted 1 : 20 in sterile PBS). After three washes with PBS, coverslips were mounted on microscope slides with Eukitt (Bio-Optica) and analyzed with an Eclipse Ni-U microscope (Nikon, Tokyo, Japan) equipped with a DS-SM-L1 digital camera (Nikon).

Differential hemocyte counts were performed by using hemolymph of control larvae and larvae injected with bacteria or chromatographic beads, after Giemsa staining. Cells from 10 randomly selected fields (50 \times magnification) were counted. At least 20 cells for each cell type were considered for size determination. Differential hemocyte counts were expressed as the percentage of each hemocyte type from the total number of cells counted (Silva *et al.*, 2002). Each experiment was performed in triplicate.

Identification of crystal cells Crystal cells were identified by evaluating their melanization activity (Corcoran & Brückner, 2020). For this purpose, naïve larvae and larvae injected with bacteria or chromatographic beads were placed in 2-mL plastic tubes with sterile PBS and then heated at 65 °C for 22 min in a Thermomixer comfort (Eppendorf, Hamburg, Germany) (Corcoran & Brückner, 2020). Hemolymph was then collected, diluted (2 : 1 v/v) with Schneider's Insect Medium (Merck), and placed in a 96-well plate. Cells undergoing melanization were identified by using an inverted Olympus IX51 micro-

scope (Olympus, Tokyo, Japan) equipped with a C-P20M camera (Optika Microscopes Italia, Ponteranica, Italy).

Identification and quantification of adipohemocytes Adipohemocytes were identified and quantified by using an osmium staining protocol adapted from Belazi *et al.* (2009). Hemocytes were isolated from naïve larvae and larvae injected with bacteria or chromatographic beads, poured on sterile round glass coverslips as described in "Giemsa staining and differential hemocyte counts" to allow adherence, and then fixed with 5% formalin in distilled water (v/v) for 10 min in the dark. Coverslips were washed with PBS and then incubated with 1% osmium tetroxide in PBS (v/v) for 1 min in the dark. They were repeatedly washed with distilled water and dehydrated with an ascending ethanol series. Finally, coverslips were mounted on microscope glass slides with Eukitt (Bio-Optica) and analyzed with an Eclipse Ni-U microscope (Nikon) equipped with a DS-SM-L1 digital camera (Nikon). Adipohemocytes were quantified by analyzing 10 different images (50 \times magnification) randomly selected from each independent experiment. Each experiment was performed in triplicate.

Transmission electron microscopy Hemocytes were fixed by mixing 1 mL of hemolymph with 2% glutaraldehyde in 0.1 mol/L sodium cacodylate buffer (1 : 1, v/v), pH 7.4, overnight at 4°C. After centrifuging at 200 \times g for 10 min, cell pellets were postfixed in 2% osmium tetroxide in 0.1 mol/L sodium cacodylate buffer for 20 min at room temperature in the dark. Samples were then dehydrated in an ascending ethanol series and embedded in an Epon-Araldite 812 mixture. Ultrathin sections (70 nm thick) were obtained with Leica Reichert Ultracut S (Leica, Wetzlar, Germany) and stained with lead citrate and uranyl citrate. Specimens were observed with a JEM-1010 TEM (Jeol, Tokyo, Japan) equipped with a Morada digital camera (Olympus)—Centro Grandi Attrezzature, University of Insubria.

Immunocytochemistry After adhesion on sterile round glass coverslips as described in "Giemsa staining and differential hemocyte counts," hemocytes were fixed in 4% paraformaldehyde in PBS for 10 min at room temperature. Then, coverslips were washed with PBS. Preincubation with blocking solution (2% bovine serum albumin [BSA] with 0.01% Tween-20 in PBS) for 30 min preceded incubation with a rabbit anti-phospho-Histone 3 antibody ([#06-570, Merck], dilution 1 : 500 in 2% PBS/BSA [v/w] with 0.01% Tween-20) for 1 h at room temperature. This antibody is able to recognize mitotic cells in *H. illucens* (Bonelli *et al.*, 2019). After several washes with PBS, cells were incubated with an

anti-rabbit Cy3-conjugated secondary antibody (dilution 1 : 300 in 2% PBS/BSA [v/w] with 0.01% Tween-20) (Abcam, Cambridge, UK) for 1 h at room temperature. After several washes with PBS, hemocytes were incubated with DAPI (100 ng/mL in PBS) for 5 min to stain nuclei and then mounted with Citifluor (Citifluor Ltd, London, UK). Specimens were analyzed with an Eclipse Ni-U microscope (Nikon) equipped with a DS-SM-L1 digital camera (Nikon). Phospho-histone 3-positive cells were quantified by analyzing 10 different images (50× magnification) randomly selected from each independent experiment. The experiments were conducted in triplicate. Negative controls were performed by omitting the primary antibody.

Flow cytometry analysis of apoptotic cells Apoptotic cells in the hemolymph of naïve and infected larvae were quantified by flow cytometry. Here, 1 mL of hemolymph was collected from 50 larvae 30 min, 1 h, and 2 h after injecting the bacteria. Samples were then centrifuged at $200 \times g$ for 10 min. The pellets were washed three times with sterile PBS, fixed in cold 70% ethanol, and stored at -20°C until use. For FACS analysis, cells were centrifuged for 10 min at $1100 \times g$ and DNA was stained with 250 μL of 50 $\mu\text{g/mL}$ propidium iodide in PBS in the presence of 30 U/mL of RNase A. Samples were analyzed with a FACSCalibur flow cytometer and data were processed using CELLQUESTPRO software (Becton Dickinson, Franklin Lakes, NJ, USA). Fluorescence emission of propidium iodide was collected through a 575-nm band-pass filter, acquired in logarithmic mode, and the percentage of apoptotic cells was determined based on sub-G1 peaks detected in monoparametric histograms (Riccardi & Nicoletti, 2006). The analyses were conducted in triplicate for each time-point analyzed.

PLA2 activity and PGE₂ quantification Activity of PLA2 and quantification of PGE₂ were assessed in both cell-free and total hemolymph samples collected from uninfected and infected larvae at 30 min and 3 h after infection. After isolation, hemolymph samples were diluted with Schneider's Insect Medium (Merck) (4 : 1 ratio) and a few crystals of *N*-phenylthiourea (Sigma-Aldrich, St Louis, MO, USA) were added to the solution to avoid proPO activation. Cell-free hemolymph samples were obtained by centrifuging the hemolymph at $10\,000 \times g$ for 10 min at 4°C . However, total hemolymph samples were first sonicated for 3 min for cell lysis and then centrifuged at $10\,000 \times g$ for 10 min at 4°C . Supernatants were collected and stored at -80°C until use.

The PLA2 activity was detected by using the fluorometric EnzChek Phospholipase A2 Assay Kit (Invitrogen, Carlsbad, CA, USA), which provides sensitive and rapid real-time monitoring of PLA2 activity. Briefly, the hemolymph samples were diluted 1 : 5 with the reaction buffer to ensure that conditions were appropriate for the enzymatic reaction. Measurements were performed using the fluorescence endpoint method (excitation: 485/20 nm, emission: 528/20 nm) with a Synergy HT Multi-Mode Microplate Reader (BioTek, Winooski, VT, USA). Quantitative eicosanoid analysis was carried out using the Human Prostaglandin E₂ Elisa Kit (Bioassay Technology Laboratory, Shanghai, China). Absorbance (wavelengths: 450 nm) was measured using a Synergy HT Multi-Mode Microplate Reader (BioTek). PLA2 activity and PGE₂ concentration were assessed by means of their respective standard curves. Each test was performed in three independent replicates according to the manufacturer's instructions.

Statistical analysis

Statistical analysis was performed using GRAPHPAD PRISM version 7.00 (GraphPad software, La Jolla, CA, USA). Quantification of apoptotic cells and PGE₂ over time, PLA2 activity, as well as the variation in numbers of adipohemocytes, granulocytes, and crystal cells under different conditions (i.e., control larvae and larvae injected with the bacterial mix or chromatographic beads) were analyzed using one-way analysis of variance followed by Tukey's multiple-comparison post hoc test. Hemocyte counts and mitotic hemocytes were analyzed using the unpaired Student's *t*-test. The normality of all the data was checked and confirmed with the Shapiro-Wilk test. Differences between groups were considered statistically significant at a *P* value less than 0.05.

Results

Morphological characterization of hemocytes

Five different types of hemocytes were identified in naïve larvae according to their morphology and appearance after Giemsa staining, namely: prohemocytes, plasmatocytes, lamellocyte-like cells, crystal cells, and granulocytes (Fig. 1A–E). As reported in Table 1, plasmatocytes represented the most abundant population, corresponding to 91% of circulating cells in the hemolymph. A smaller fraction of hemocytes (about 7%) was represented by prohemocytes, whereas the remaining cell types amounted to less than 1% each. Immature

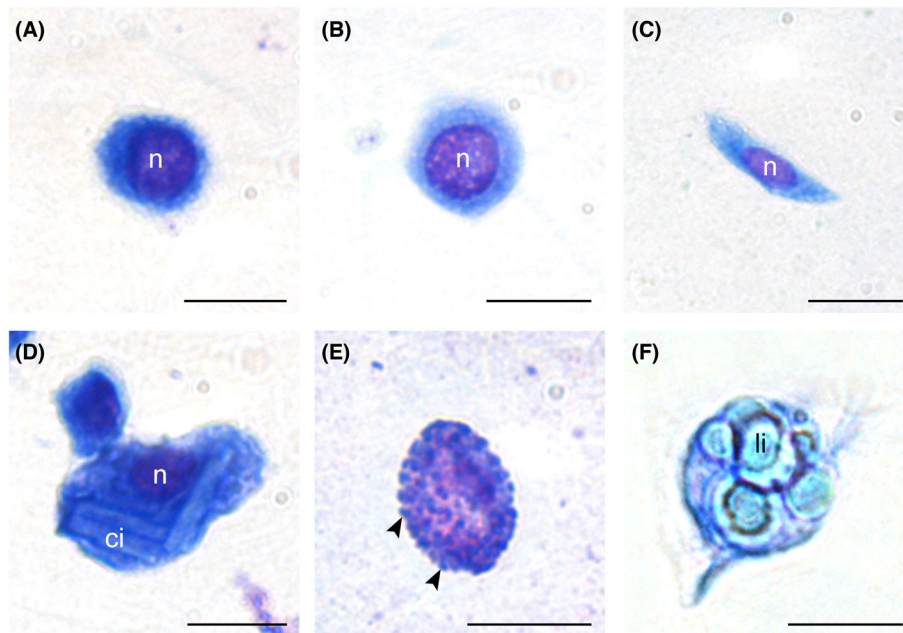


Fig. 1 Morphological characterization of hemocytes—light microscopy. (A) Prohemocyte; (B) plasmatocyte; (C) lamellocyte-like cell; (D) crystal cell; (E) granulocyte; (F) adipohemocyte. Arrowheads: granules; ci: crystalline inclusion; li: lipid inclusion; n: nucleus. Bars: 5 μm (A), 10 μm (B–F).

Table 1 Relative percentages and dimensions of the hemocyte types in naïve larvae.

Hemocytes	Percentage	Dimensions (μm)
Plasmatocytes	90.90 ± 1.50	9 ± 0.4
Prohemocytes	6.82 ± 0.53	5 ± 0.6
Granulocytes	0.09 ± 0.04	9 ± 0.5
Crystal cells	0.38 ± 0.24	18 ± 0.8
Lamellocyte-like cells	0.70 ± 0.59	Length 16 ± 0.9 , Width 4 ± 0.3
Not determined	1.11 ± 0.27	13 ± 0.6

Values represent mean \pm SEM. At least 20 cells for each cell type were analyzed for size determination.

hemocytes and intermediate figures, not classifiable in any of the previous morphotypes, represented about 1% of circulating cells.

Ultrastructural analysis showed that prohemocytes were round or oval cells with a high nucleus : cytoplasm ratio (Fig. 2A, B). A thin, homogeneous layer of cytoplasm almost devoid of rough endoplasmic reticulum (RER) and mitochondria surrounded the centrally located nucleus (Fig. 2B). Plasmatocytes were, in contrast, rich in organelles, as a well-developed RER, numerous mitochondria, and lysosomes (Fig. 2C, D). These cells showed a lobed, eccentrically located nucleus as well as numerous membrane protrusions (Fig. 2C). Lamellocyte-like cells were elongated in shape with tapered ends, with a large oval nucleus and a developed RER (Fig. 2E, F).

Crystal cells were the largest hemocytes in naïve larvae (Fig. 2G, H) (Table 1). They were characterized by numerous, large crystalline inclusions in the cytoplasm that could extend throughout the cell (Fig. 2H), a large, round nucleus, and a smooth membrane without protrusions (Fig. 2G, H). Finally, granulocytes were spherical in shape (Fig. 2I). They were characterized by an irregular membrane, a centrally located, lobed nucleus, and spherical or ovoidal electron-dense granules in the cytoplasm (Fig. 2I, J). The dimensions of all the hemocyte types observed in naïve larvae are reported in Table 1. Interestingly, a sixth cell type, i.e., adipohemocytes, was detected only in larvae subjected to immune challenge (Figs. 1F and 2K, L). These round or oval cells were large ($16 \pm 1.2 \mu\text{m}$; $n = 10$), with a round or slightly

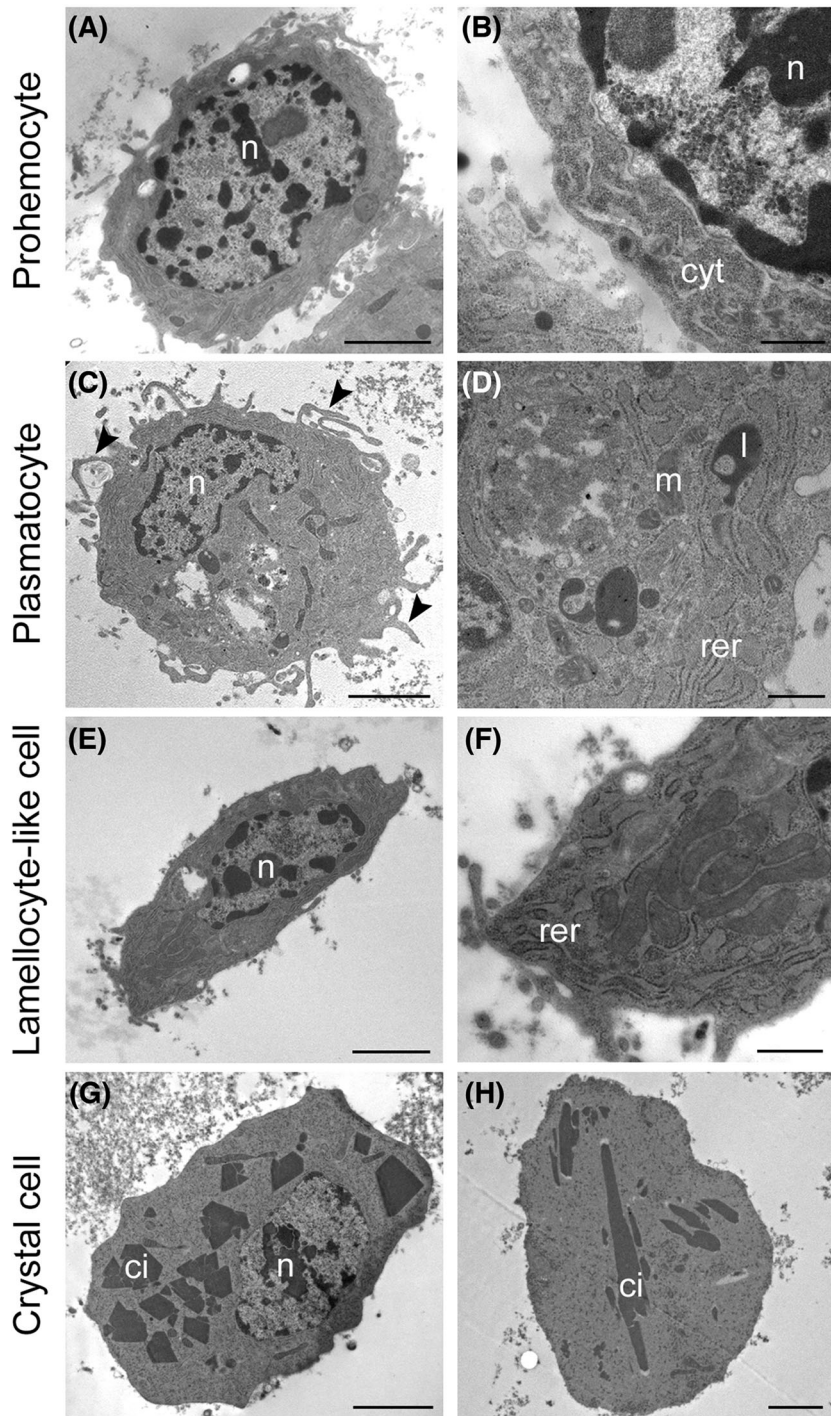


Fig. 2 Morphological characterization of hemocytes—transmission electron microscopy. (A, B) Prohemocyte; the cell is characterized by a high nucleus : cytoplasm ratio. (C, D) Plasmatocyte; the lobed nucleus (n), numerous pseudopodia (arrowheads), and lysosomes (l) are visible. (E, F) Lamellocyte-like cell; the typical elongated shape of the cell and developed rough endoplasmic reticulum can be observed. (G, H) Crystal cell; the large nucleus (n) and peculiar crystalline inclusions (ci) in the cytoplasm are visible. (I, J) Granulocyte; numerous electron-dense granules (g) are present in the cytoplasm. (K, L) Adipohemocyte; a large amount of lipid inclusions (li) can be observed in the cytoplasm. cyt: cytoplasm; m: mitochondria; rer: rough endoplasmic reticulum; v: vacuoles. Bars: 2 μm (A, C, E, G, H, I, K, L), 500 nm (B, D, F, J).

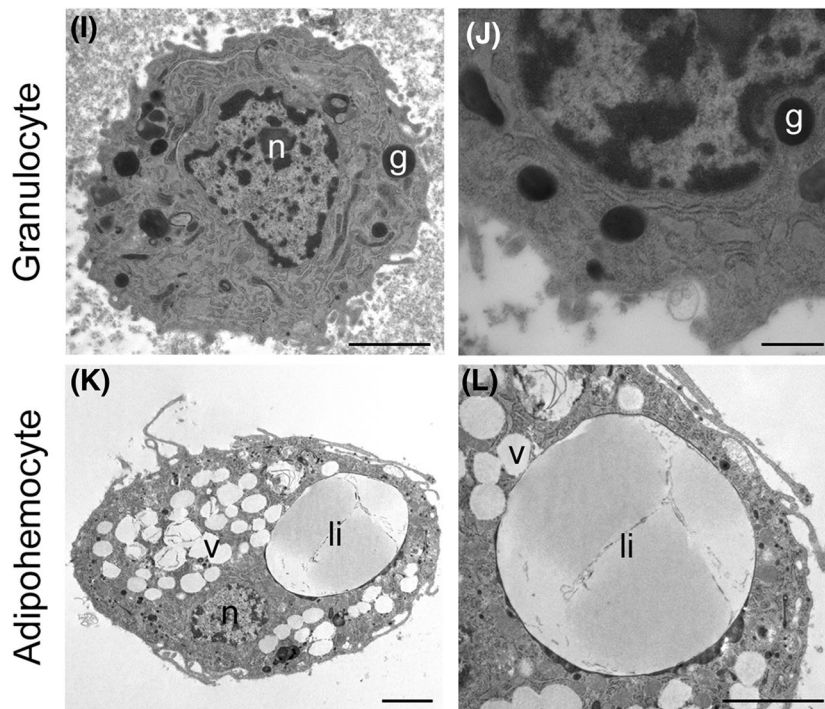


Fig. 2 *Continued*

elongated, small nucleus, located eccentrically (Fig. 2K). Their membrane was irregular and characterized by thin protrusions. Numerous lipid droplets and vacuoles were present in the cytoplasm (Fig. 2L).

Activation of hemocytes by immune challenge: phagocytosis, nodulation, and encapsulation

Hemocyte-mediated processes were evaluated by challenging larvae with bacteria and different types of beads (Figs. 3 and 4).

Phagocytosis was analyzed within a short time after infection, i.e., within 1 h after injection of bacteria (Bruno *et al.*, 2021). Morphological changes in hemocytes confirmed the rapid activation of this cell-mediated process. In particular, numerous membrane protrusions (Fig. 3A) as well as engulfed bacteria (Fig. 3B, E, F) were frequently observed in activated plasmatocytes, from 5 to 15 min after infection. Moreover, phagolysosomes containing degraded bacteria were detected in their cytoplasm within 30 min (Fig. 3C, G). Interestingly, phagocytosis was accompanied by a rapid removal of exhausted hemocytes. In particular, apoptotic cells, clearly recognizable for cytoplasm vacuolization and chromatin condensation (Fig. 3D, H), could be observed as freely circulating cells (Fig. 3D) or engulfed by phagocytes (Fig. 3H) 1 h after infection. These results were confirmed by

FACS analysis. In detail, apoptotic hemocytes detected 1 h after infection were significantly more abundant than in naïve larvae at all the time-points (Fig. 5A).

Large bacterial aggregates that could not be phagocytosed soon after infection (10 min) were removed by nodulation (Fig. 3I), as confirmed by plasmatocytes surrounding clusters of bacteria through pseudopodia and melanin presence within the nodule (Fig. 3J).

To analyze encapsulation, neutrally charged B-Agarose beads and positively charged DEAE-Sephadex beads were injected into the larvae and examined 24 h later. At this time-point, these beads are encapsulated to a different extent in BSF larvae (the former are only partially surrounded by hemocytes, whereas the latter are fully encapsulated and melanized) (Bruno *et al.*, 2021). Hence, this approach allowed us to investigate which hemocyte populations were involved in encapsulating the two non-self macroagents. Plasmatocytes, granulocytes, and presumably lamellocyte-like cells were involved in forming a compact cell capsule surrounding DEAE-Sephadex beads (Fig. 4A, B) with a typical arrangement: plasmatocytes and lamellocyte-like cells were localized in the inner part of the capsule, adherent to the foreign body (Fig. 4A, C), whereas granulocytes were distributed in the outer region (Fig. 4B, D). Moreover, encapsulated beads became completely melanized (Fig. 4E). In contrast, just a few hemocytes surrounded B-Agarose beads (Fig. 4G).

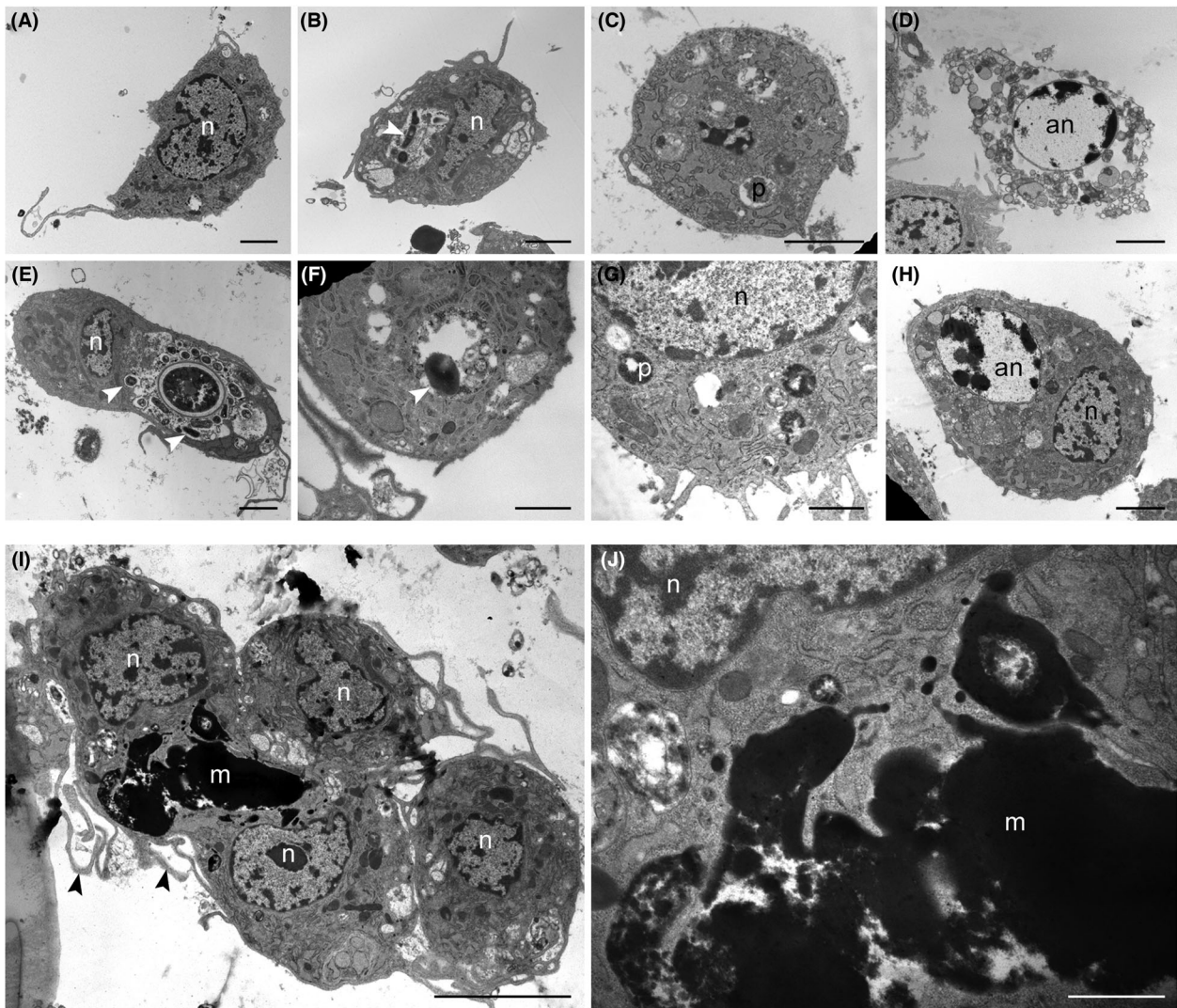


Fig. 3 Phagocytosis and nodulation. (A–H) Transmission electron microscopy analysis of plasmacytes undergoing phagocytosis of bacteria at 5–15 min (A, B, E, F) and 30 min (C, G). Circulating (D) and engulfed (H) apoptotic cells are visible 60 min after the infection. (I, J) Transmission electron microscopy analysis of plasmacytes involved in nodulation. Protrusions of the cell membrane (black arrowheads) and melanin deposition (m) are visible. an: apoptotic nucleus; n: nucleus; p: phagolysosome; white arrowheads: engulfed bacteria. Bars: 2 μm (A–E, H), 1 μm (F, G, J), 5 μm (I).

As for the DEAE-Sephadex beads, plasmacytes and granulocytes participated in encapsulation (Fig. 4G, H), but neither a fully formed cell capsule nor melanization was observed.

Morphofunctional features of activated hemocytes

To evaluate a potential turnover of exhausted hemocytes removed from hemolymph following phagocytosis (Fig. 3D, H), we compared the numbers of hemocytes in naïve and infected larvae over time. As shown in Fig. 5B,

a striking reduction in hemocytes was recorded 30 min after infection ($1.59 \times 10^6 \pm 0.08 \times 10^6$ cells/mL in naïve larvae and $6.58 \times 10^5 \pm 0.82 \times 10^5$ cells/mL in infected larvae). This decrease in cell number was maintained up to 1 h ($1.82 \times 10^6 \pm 0.15 \times 10^6$ cells/mL in naïve larvae and $7.98 \times 10^5 \pm 0.88 \times 10^5$ cells/mL in infected larvae), whereas 3 h after infection, the number of circulating cells was comparable to controls at the same time-point ($1.31 \times 10^6 \pm 0.04 \times 10^6$ cells/mL in naïve larvae and $1.17 \times 10^6 \pm 0.05 \times 10^6$ cells/mL in infected larvae), indicating a recovery in the number

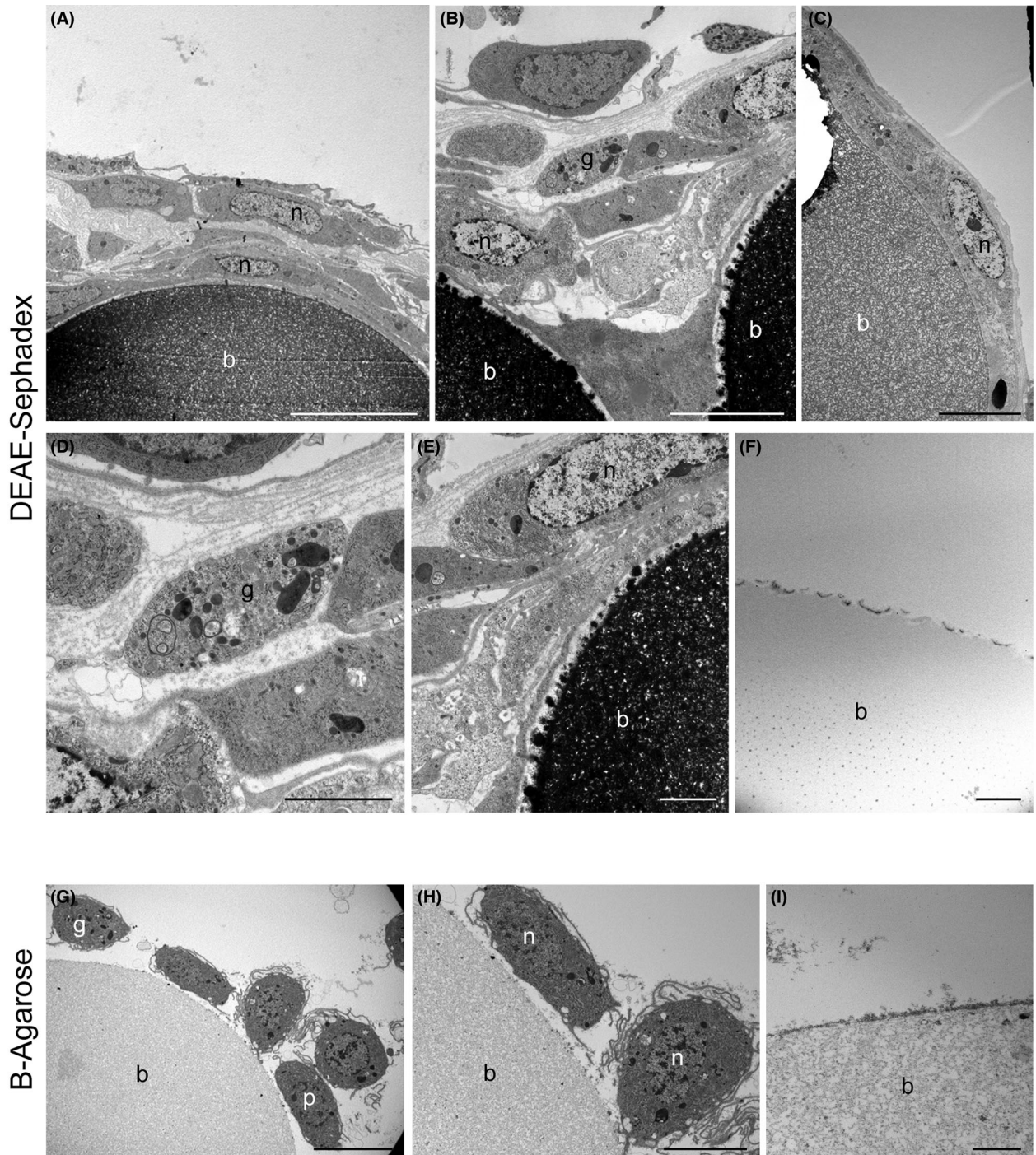


Fig. 4 Encapsulation. Transmission electron microscopy analysis of the encapsulation process 24 h after injecting DEAE-Sephadex (A–E) and B-Agarose (G, H) beads. (F, I) Morphology of control DEAE-Sephadex (F) and B-Agarose (I) beads. b: bead; g: granulocyte; n: nucleus; p: plasmatocyte. Bars: 10 μ m (A, G), 5 μ m (B, C, H), 2 μ m (D–F, I).

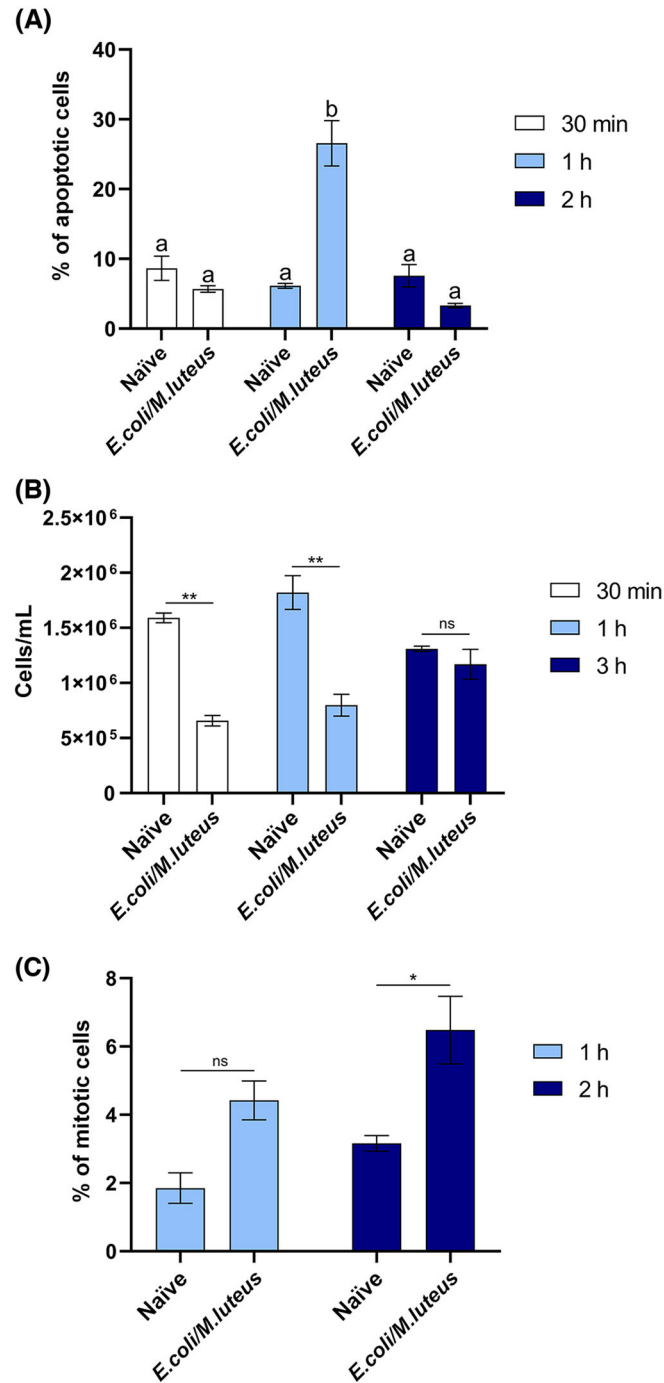


Fig. 5 Hemocyte turnover during bacterial infection. (A) Flow cytometry analysis of apoptotic hemocytes. Values represent mean \pm SEM. Different letters indicate statistically significant differences among different samples (one-way analysis of variance [ANOVA]: $F_{5-11} = 19.01$, ANOVA $P < 0.0001$; Tukey's test P values: Naïve 30 min vs. *E. coli/Micrococ luteus* 30 min $P = 0.9472$; Naïve 30 min vs. Naïve 1 h $P = 0.9734$; Naïve 30 min vs. *E. coli/M. luteus* 1 h $P = 0.0019$; Naïve 30 min vs. Naïve 2 h $P = 0.9997$; Naïve 30 min vs. *E. coli/M. luteus* 2 h $P = 0.639$; *E. coli/M. luteus* 30 min vs. Naïve 1 h $P > 0.9999$; *E. coli/M. luteus* 30 min vs. *E. coli/M. luteus* 1 h $P = 0.0002$; *E. coli/M. luteus* 30 min vs. Naïve 2 h $P = 0.9921$; *E. coli/M. luteus* 30 min vs. *E. coli/M. luteus* 2 h $P = 0.9667$; Naïve 1 h vs. *E. coli/M. luteus* 1 h $P = 0.0002$; Naïve 1 h vs. Naïve 2 h $P = 0.9978$; Naïve 1 h vs. *E. coli/M. luteus* 2 h $P = 0.9326$; *E. coli/M. luteus* 1 h vs. Naïve 2 h $P = 0.0012$; *E. coli/M. luteus* 1 h vs. *E. coli/M. luteus* 2 h $P < 0.0001$; Naïve 2 h vs. *E. coli/M. luteus* 2 h $P = 0.806$). (B) Total count of hemocytes in naïve (Naïve) and infected (*E. coli/M. luteus*) larvae at

of hemocytes in infected larvae at this time-point. H3P immunostaining demonstrated that this phenomenon was mainly due to cell proliferation, as the percentage of mitotic hemocytes doubled ($6.48\% \pm 0.9\%$) compared with naïve larvae ($3.16\% \pm 0.2\%$) 2 h after infection (Fig. 5C; Supporting Information Fig. S2). Moreover, at the same time-point, the number of apoptotic cells decreased to levels comparable to naïve larvae (Fig. 5A). Collectively, these results showed a strong reduction in apoptosis and the recovery of total hemocyte numbers through cell proliferation 2 h after infection, confirming a turnover of the immune cells.

We also observed significant modifications in the pattern and behavior of some hemocyte populations after the immune challenge. First, adipohemocytes started to circulate upon the entrance of foreign agents in the hemocoel. The presence of these cells in the hemolymph was demonstrated by TEM analysis (Fig. 2K) and osmium staining (Fig. 6B–D). In particular, adipohemocytes, which were never observed in naïve larvae (Fig. 6A), amounted to $7\% \pm 0.8\%$ of total hemocytes after infection with bacteria and $9.2\% \pm 0.5\%$ and $6.5\% \pm 1.1\%$ after injection of B-Agarose and DEAE-Sephadex beads, respectively (Fig. 6E). Second, crystal cells underwent a change in morphology and number after activation. TEM analysis showed a strong reduction in the amount of cytoplasmic crystals upon bacterial infection (Fig. 7B) or injection with DEAE-Sephadex beads (Fig. 7D) compared with naïve larvae (Fig. 7A) and larvae injected with B-Agarose beads (Fig. 7C). Larval heating triggered the phenoloxidase system such that we could monitor the crystal cell response under different conditions. These experiments confirmed that crystal cells from naïve and B-Agarose bead-injected larvae were black in color because of the presence of crystals in the cytoplasm that, after activation by heat treatment, led to spontaneous melanization of the cell (Fig. 7E, G), whereas the number of crystals in cells isolated from larvae injected with bacteria or DEAE-Sephadex beads (Fig. 7F, H) decreased. Moreover, while crystal cells increased from $0.38\% \pm 0.24\%$ in naïve larvae to $1.33\% \pm 0.17\%$ and $1.83\% \pm 0.15\%$ upon injection of B-Agarose and DEAE-Sephadex beads, respectively, the number of crystal cells remained unchanged after bacterial infection (Fig. 7I). Third, the number of granulocytes increased after injecting bacteria (3-fold compared with naïve larvae) and

DEAE-Sephadex or B-Agarose beads (6-fold compared with naïve larvae) (Fig. 8E). TEM analysis of these cells showed an increase in cytoplasmic granules after activation (Fig. 8B–D) compared with controls (Fig. 8A).

PLA2 activity and PGE₂ quantification

Activity of PLA2 was measured 30 min and 3 h after bacterial infection (Fig. 9A). In total hemolymph, the activity of PLA2 remained at basal levels 30 min after the infection (0.28 ± 0.01 U/mL versus 0.24 ± 0.03 U/mL in naïve larvae), whereas the enzyme was strongly activated at 3 h (0.5 ± 0.03 U/mL). No activity was recorded in cell-free hemolymph.

The PGE₂ concentration differed significantly between cell-free and total hemolymph (Fig. 9B). In addition, although the amount of prostaglandin remained constant in cell-free hemolymph, the concentration in total hemolymph increased significantly over time after the infection. Specifically, the amount of this eicosanoid increased from 30.9 ± 4.7 ng/L in naïve larvae to 50.9 ± 1.3 ng/L and to 67.2 ± 4.7 ng/L in infected larvae at 30 min and 3 h, respectively.

Discussion

In the present study, we morphofunctionally characterized the hemocyte populations in larvae of *H. illucens*, a saprophagous insect that is increasingly being used for waste bioconversion. This work also expands the current knowledge on immune cells in insects in general and confirms the high variability of hemocytes in Diptera. Indeed, except for prohemocytes and plasmatocytes, which are widely conserved among insects, two specific hemocyte populations, granulocytes and adipohemocytes, which have been previously described in the larvae of other Cyclorrhapha such as *Sarcophaga ruficornis*, *Chrysomya megacephala*, and *Musca domestica*, mount the immune response in BSF larvae (Pal & Kumar, 2014). However, no crystal cells were described in any of these Diptera, unlike *D. melanogaster* larvae (Meister & Lagueur, 2003). Hence, the profile of hemocytes in *H. illucens* seems to be unique and mixed, which is relevant for the vast majority of cyclorrhaphan Diptera, i.e., prohemocytes, plasmatocytes, granulocytes, and

different time-points. (C) Percentage of mitotic hemocytes in naïve (Naïve) and infected (*E. coli/M. luteus*) larvae at different time-points. Values represent mean \pm SEM. Asterisks represent statistically significant differences between naïve larvae (Naïve) compared with larvae injected with bacteria (*E. coli/M. luteus*) at different time-points—unpaired Student's *t* test: (B) for 30 min, $t = 8.226$, $df = 4$, $P = 0.0012$; for 1 h, $t = 5.588$, $df = 4$, $P = 0.005$; for 3 h, $t = 0.574$, $df = 4$, $P = 0.597$; (C) for 1 h, $t = 2.06$, $df = 4$, $P = 0.109$; for 2 h, $t = 3.257$, $df = 4$, $P = 0.031$).

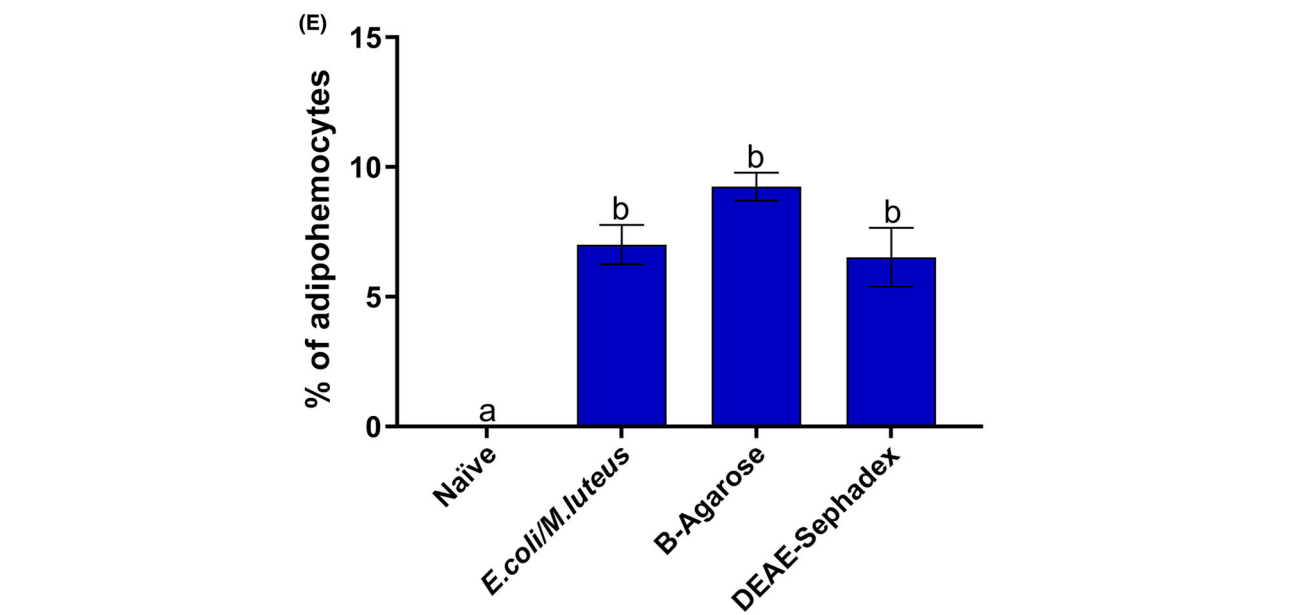
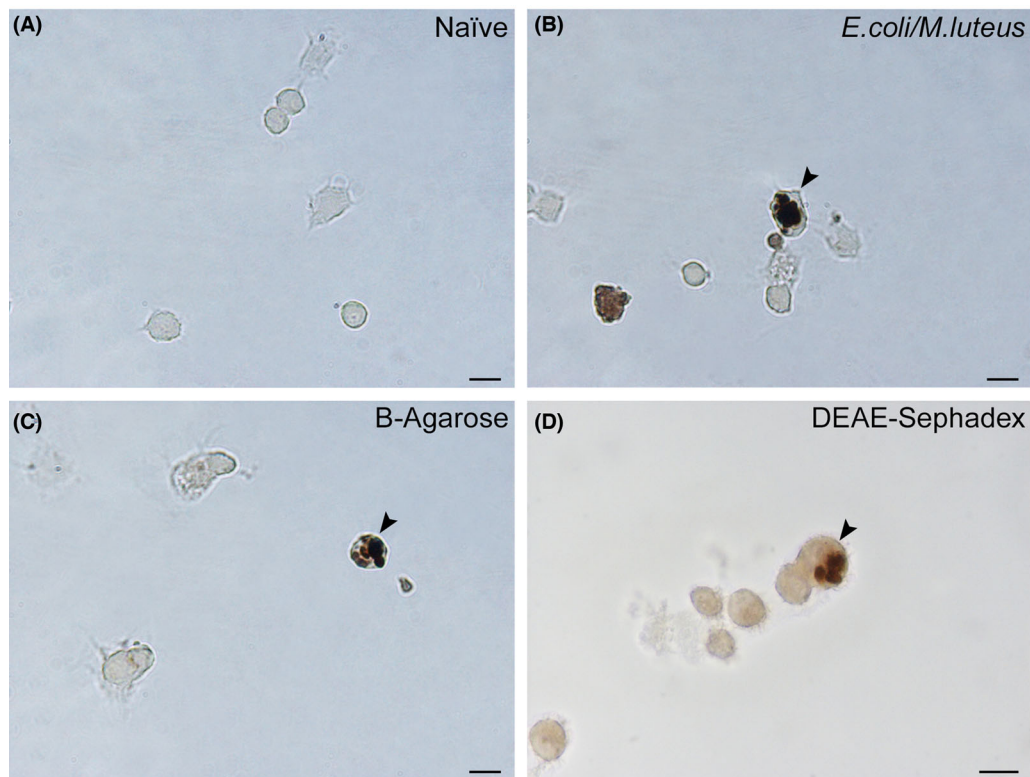


Fig. 6 Adipohemocytes. The presence of adipohemocytes (arrowheads) was investigated through osmium tetroxide staining in naïve larvae (A) and 24 h after the injection of bacteria (B), B-Agarose beads (C), and DEAE-Sephadex beads (D). (E) Quantification of circulating adipohemocytes. Values represent mean \pm SEM. Different letters indicate statistically significant differences among different samples (one-way analysis of variance [ANOVA]: $F_{3,8} = 29.3$, ANOVA $P < 0.0001$; Tukey's test P values: Naïve vs. *E. coli/M. luteus* $P = 0.0007$, Naïve vs. B-Agarose $P < 0.0001$, Naïve vs. DEAE-Sephadex $P = 0.0011$, *E. coli/M. luteus* vs. B-Agarose $P = 0.2189$, *E. coli/M. luteus* vs. DEAE-Sephadex $P = 0.9626$, B-Agarose vs. DEAE-Sephadex $P = 0.1141$). Bars: 10 μ m.

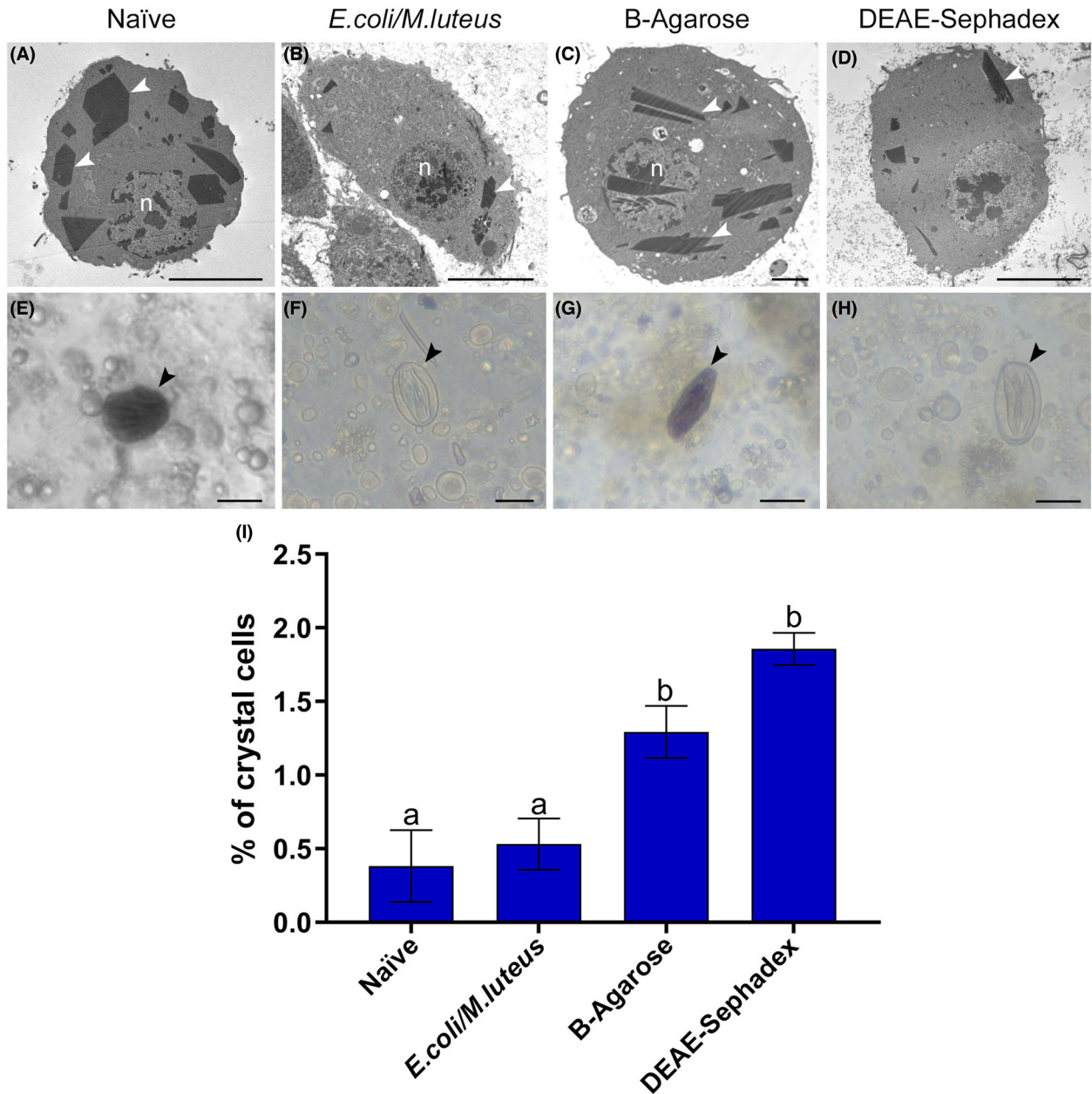


Fig. 7 Crystal cells. (A–D) Transmission electron microscopy analysis of crystal cells in naïve larvae (A) and larvae 24 h after injecting bacteria (B), B-Agarose beads (C), and DEAE-Sephadex beads (D). (E–H) Evaluation of phenoloxidase (PO) activation in crystal cells of naïve larvae (E) and larvae 24 h after injecting bacteria (F), B-Agarose beads (G), and DEAE-Sephadex beads (H). (I) Quantification of circulating crystal cells. Values represent mean \pm SEM. Different letters indicate statistically significant differences among different samples (one-way analysis of variance [ANOVA]: $F_{3,7} = 19.35$, ANOVA $P = 0.0009$; Tukey's test P values: Naïve vs. *E. coli/M. luteus* $P = 0.9183$, Naïve vs. B-Agarose $P = 0.0219$, Naïve vs. DEAE-Sephadex $P = 0.0018$, *E. coli/M. luteus* vs. B-Agarose $P = 0.0294$, *E. coli/M. luteus* vs. DEAE-Sephadex $P = 0.0017$, B-Agarose vs. DEAE-Sephadex $P = 0.1311$). Black arrowheads: crystal cells; n: nucleus; white arrowheads: crystalline inclusions. Bars: 5 μm (A, B, D), 2 μm (C), 10 μm (E–H).

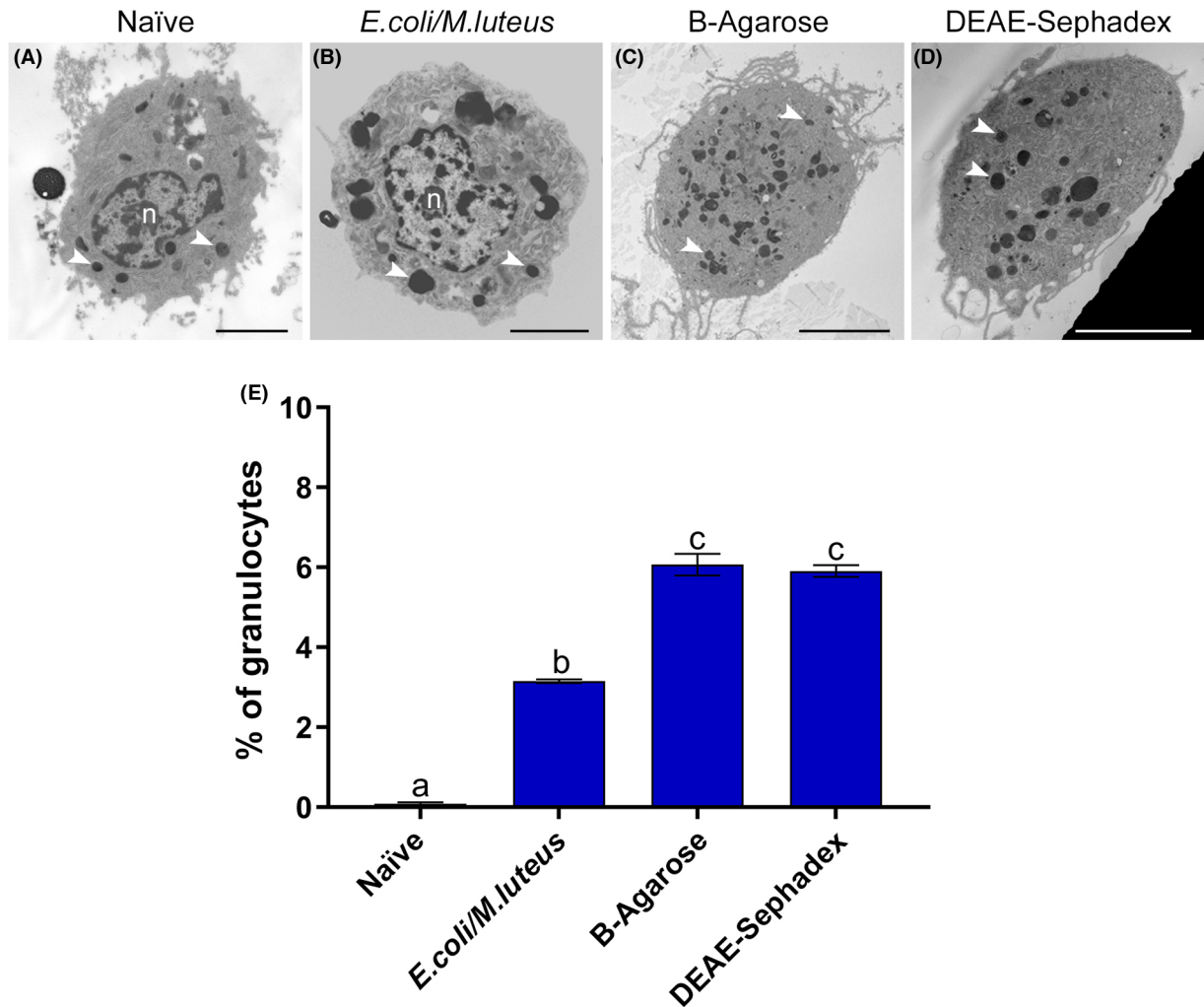


Fig. 8 Granulocytes. Transmission electron microscopy analysis of granulocytes in naïve larvae (A) and larvae 24 h after injecting bacteria (B), B-Agarose beads (C), and DEAE-Sephadex beads (D). (E) Quantification of circulating granulocytes. Values represent mean \pm SEM. Different letters indicate statistically significant differences among different samples (one-way analysis of variance [ANOVA]: $F_{3,7} = 74.34$, ANOVA $P < 0.0001$; Tukey's test P values: Naïve vs. *E. coli/M. luteus* $P = 0.0009$, Naïve vs. B-Agarose $P < 0.0001$, Naïve vs. DEAE-Sephadex $P < 0.0001$, *E. coli/M. luteus* vs. B-Agarose $P = 0.0011$, *E. coli/M. luteus* vs. DEAE-Sephadex $P = 0.0016$, B-Agarose vs. DEAE-Sephadex $P = 0.9778$). Arrowheads: granules; n: nucleus. Bars: 2 μm (A), 5 μm (B, C, D).

adipohemocytes (Kaaya & Ratcliffe, 1982; Silva *et al.*, 2002; Pal & Kumar, 2014; Dorrah *et al.*, 2019). It differs, however, in the presence of the crystal cells, analogous to that of *Drosophila* (Meister & Lagueux, 2003), and in the complete absence of spherulocytes and the enigmatic oenocytoids relevant for other Diptera such as mosquitoes (Castillo *et al.*, 2006; Araújo *et al.*, 2008).

We showed that the number of circulating hemocytes in BSF larvae undergoes a marked reduction within 1 h after infection, as in other insects (Kaaya *et al.*, 1986; Li *et al.*, 2019). TEM analysis suggests that this is probably due to the removal of exhausted hemocytes by

circulating phagocytic cells, as hypothesized for *Bombyx mori* (Li *et al.*, 2019). The total number of hemocytes increases again 2 h later, reaching levels comparable to those in control larvae, providing new immune cells to better cope with the infection. This phenomenon can be explained by one of the following mechanisms, or a combination thereof: (i) proliferation of circulating hemocytes, as indicated by H3P immunostaining; (ii) mobilization, following infection, of specific hemocytes (i.e. adipohemocytes) which under healthy conditions adhere to tissues or organs (Hillyer & Christensen, 2002); and (iii) *ex novo* production by hematopoietic organs of

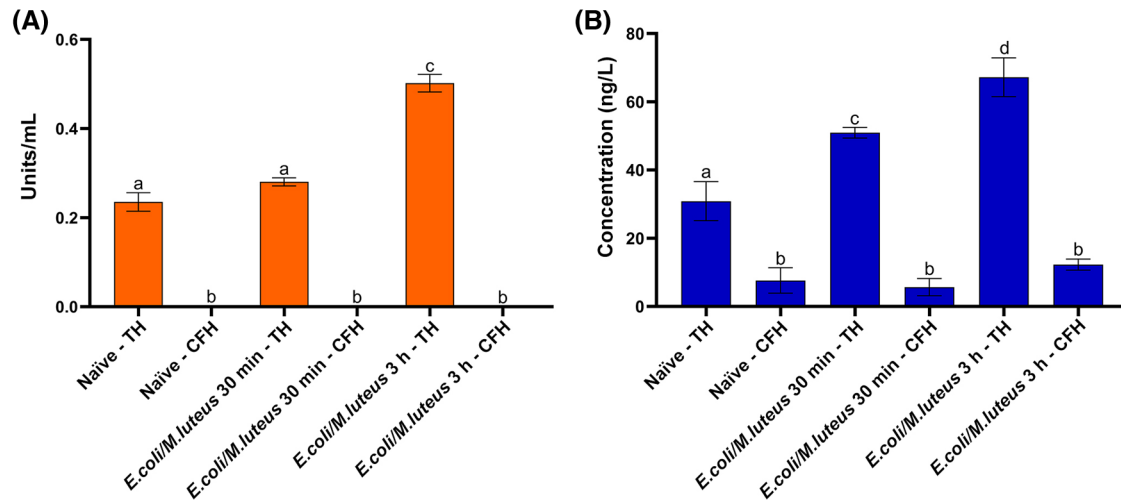


Fig. 9 Phospholipase A2 (PLA2) activity and prostaglandin E₂ (PGE₂) production. Activity of PLA2 (A) and quantification of PGE₂ (B) in total hemolymph (TH) and cell-free hemolymph (CFH) of naïve larvae (Naïve) and larvae at 30 min and 3 h after bacterial infection (*E.coli/M.luteus*). Values represent mean \pm SEM. Different letters indicate statistically significant differences among the different samples at different time-points (one-way analysis of variance [ANOVA]). (A) $F_{5-12} = 284.5$, ANOVA $P < 0.0001$; Tukey's test P values: Naïve - TH vs. Naïve - CFH $P < 0.0001$, Naïve - TH vs. *E. coli/M. luteus* 30 min - CFH $P < 0.0001$, Naïve - TH vs. *E. coli/M. luteus* 3 h - TH $P < 0.0001$, Naïve - TH vs. *E. coli/M. luteus* 3 h - CFH $P < 0.0001$, Naïve - CFH vs. *E. coli/M. luteus* 30 min - TH $P < 0.0001$, Naïve - CFH vs. *E. coli/M. luteus* 30 min - CFH $P > 0.9999$, Naïve - CFH vs. *E. coli/M. luteus* 3 h - TH $P < 0.0001$, Naïve - CFH vs. *E. coli/M. luteus* 3 h - CFH $P > 0.9999$, *E. coli/M. luteus* 30 min - TH vs. *E. coli/M. luteus* 30 min - CFH $P < 0.0001$, *E. coli/M. luteus* 30 min - TH vs. *E. coli/M. luteus* 3 h - TH $P < 0.0001$, *E. coli/M. luteus* 30 min - TH vs. *E. coli/M. luteus* 3 h - CFH $P < 0.0001$, *E. coli/M. luteus* 30 min - CFH vs. *E. coli/M. luteus* 3 h - TH $P < 0.0001$, *E. coli/M. luteus* 30 min - CFH vs. *E. coli/M. luteus* 3 h - CFH $P > 0.9999$, *E. coli/M. luteus* 3 h - TH vs. *E. coli/M. luteus* 3 h - CFH $P < 0.0001$. (B) $F_{5-12} = 128.1$, ANOVA $P < 0.0001$; Tukey's test P values: Naïve - TH vs. Naïve - CFH $P = 0.0001$, Naïve - TH vs. *E. coli/M. luteus* 30 min - TH $P = 0.0004$, Naïve - TH vs. *E. coli/M. luteus* 30 min - CFH $P < 0.0001$, Naïve - TH vs. *E. coli/M. luteus* 3 h - TH $P < 0.0001$, Naïve - TH vs. *E. coli/M. luteus* 3 h - CFH $P = 0.0008$, Naïve - CFH vs. *E. coli/M. luteus* 30 min - TH $P < 0.0001$, Naïve - CFH vs. *E. coli/M. luteus* 30 min - CFH $P = 0.9876$, Naïve - CFH vs. *E. coli/M. luteus* 3 h - TH $P < 0.0001$, Naïve - CFH vs. *E. coli/M. luteus* 3 h - CFH $P = 0.6892$, *E. coli/M. luteus* 30 min - TH vs. *E. coli/M. luteus* 30 min - CFH $P < 0.0001$, *E. coli/M. luteus* 30 min - TH vs. *E. coli/M. luteus* 3 h - TH $P = 0.0026$, *E. coli/M. luteus* 30 min - TH vs. *E. coli/M. luteus* 3 h - CFH $P < 0.0001$, *E. coli/M. luteus* 30 min - CFH vs. *E. coli/M. luteus* 3 h - TH $P < 0.0001$, *E. coli/M. luteus* 30 min - CFH vs. *E. coli/M. luteus* 3 h - CFH $P = 0.3556$, *E. coli/M. luteus* 3 h - TH vs. *E. coli/M. luteus* 3 h - CFH $P < 0.0001$.

prohemocytes, which generate mature hemocytes (Jung et al., 2005).

We previously showed that hemocytes already circulating in healthy BSF larvae induce phagocytosis, nodulation, and encapsulation as soon as the infection begins (Bruno et al., 2021). As demonstrated in this study, phagocytosis is triggered within a few minutes. Although the kinetics is similar to that in other Diptera (Hillyer et al., 2003a), ultrastructural analysis indicates that only plasmatocytes participate in this process in BSF. This peculiar feature is shared by *H. illucens* and *D. melanogaster* larvae (Meister & Lagueux, 2003), but it differs from other Cyclorrhapha, where phagocytosis is mediated by both plasmatocytes and granulocytes (Franchini et al., 1996) or preferentially by the latter (Faraldo & Lello, 2003), and Nematocera (i.e.

mosquitoes) in which granulocytes engulf bacteria (Hillyer et al., 2003a; Hillyer et al., 2003b; Castillo et al., 2006; Smith et al., 2016). When we extend the comparison to other holometabolous insects, plasmatocytes have never been described, to the best of our knowledge, as the only phagocytic hemocytes. In many lepidopteran species (i.e. *Heliothis armigera*, *Galleria mellonella*, *Spodoptera littoralis*, and *B. mori*), for example, the major phagocytic activity has been attributed to granulocytes (Salama & Sharaby, 1985; Tojo et al., 2000; Costa et al., 2005; Wu et al., 2015), whereas in Coleoptera, both oenocytoids and granulocytes act as phagocytes (Giulianini et al., 2003). Hence, it seems that *H. illucens* larvae, where different populations of hemocytes developed, experienced a strong functional specialization during evolution, at least for phagocytosis.

In contrast to phagocytosis, the type and role of hemocytes involved in encapsulating large foreign agents are highly conserved among insects (Lavine & Strand, 2002). Generally, granulocytes intervene first and release granules to chemoattract plasmatocytes toward the foreign agent (Pech & Strand, 1996), which is progressively surrounded by these cells in a multilayered capsule that can eventually be melanized (Gorman *et al.*, 1998). The cell pattern observed in BSF during encapsulation is comparable to that reported in other insects and, although we were not able to definitely distinguish plasmatocytes from lamellocytes, our results suggest that, in addition to plasmatocytes, also lamellocyte-like cells are likely involved in capsule formation, as demonstrated in *D. melanogaster* larvae (Rizki & Rizki, 1992). The presence of granulocytes close to both types of beads indicates their active involvement in encapsulation. Moreover, the high number of circulating granulocytes when encapsulation has already been completed (24 h after bead injection), as well as the large number of granules in their cytoplasm, suggest that these cells could help to mount a faster immune response in the case of repeated infections. The increase in granules after injecting both types of beads and the melanization of DEAE-Sephadex beads only indicate that granulocytes are primarily involved in recruiting hemocytes that participate in capsule formation and not in the production of proPO, as in *G. mellonella* (Schmit *et al.*, 1977). In *H. illucens*, this zymogen can instead be synthesized by crystal cells (Paro & Imler, 2016), as demonstrated by the large cytoplasmic crystalline inclusions containing enzymes for melanization (Meister, 2004) and by heating assays. These results also demonstrate that, differently from *Drosophila* (Bidla *et al.*, 2007), crystal cell disruption does not occur in BSF as crystals are likely dissolved progressively in these larvae and their content is released into the hemolymph. In addition, the increase in crystal cells involved in encapsulation over time can support the melanization of nonself agents, as in parasitized *D. melanogaster* larvae (Sorrentino *et al.*, 2002). Crystal cells likely intervene in nodulation, too, whereby melanin is deposited in the nodule formed by plasmatocytes (Satyavathi *et al.*, 2014). In this case, the process could be triggered by granulocytes, which significantly increase in number upon bacterial infection by releasing their granules and favoring agglutination of bacteria, thus recruiting plasmatocytes and crystal cells (Dean *et al.*, 2004).

As mentioned above, adipohemocytes, which adhere to inner tissues/organs in naïve larvae (Hillyer & Christensen, 2002), start circulating in the hemolymph following infection. According to this change in behavior and the high lipid content in the cytoplasm (Hwang *et al.*,

2015), we hypothesize that these cells play a trophic role toward other hemocytes engaged in the immune response. This function seems to be independent of the stimulus because no difference in their number was observed after different immune challenges.

To summarize, the cellular response in BSF larvae mediated by hemocytes is finely regulated to rapidly counteract the diffusion of foreign agents. Our results demonstrate that phagocytosis is carried out by plasmatocytes only. Granulocytes are instead involved in encapsulation and nodulation, developing a starting core for capsule/nodule formation to isolate/remove large nonself agents/bacterial aggregates from the hemolymph, respectively. Crystal cells participate in these cell-mediated processes by releasing crystals that contain proPO for melanin production. Finally, adipohemocytes likely support trophically other hemocytes during the immune response (Fig. 10).

In insects, the rapid synthesis of prostaglandins, triggered by the activation of PLA2 (Kim *et al.*, 2018), activates hemocytes, phagocytosis, and the proPO system (Mandato *et al.*, 1997; Roy & Kim, 2021). In particular, PGE₂ can mediate the occurrence of apoptosis in *G. mellonella* hemocytes (Wrońska *et al.*, 2022), hemocyte spreading (Kim *et al.*, 2020), and the release of proPO from oenocytoids in *Spodoptera exigua* (Shrestha *et al.*, 2011). Our results for PLA2 and PGE₂ indicate that eicosanoids are potentially involved as mediators of the cellular immune responses of BSF larvae against bacterial infections. This hypothesis is corroborated by the active role of hemocytes in the synthesis of prostaglandins, as shown by comparing cell-free and total hemolymph samples. Future studies are needed to dissect how PGE₂ regulates specific cell-mediated immune mechanisms in this insect.

Although recent studies aimed to identify hemocyte populations in BSF larvae, they underestimated the number, variability, and behavior of circulating hemocytes in this insect (Zdybicka-Barabas *et al.*, 2017; von Bredow *et al.*, 2021). Thanks to TEM analysis, we identified specific cell populations—some of which were not properly classified or were completely overlooked in previous studies—and defined ultrastructural features of hemocytes that have been neglected so far (Zdybicka-Barabas *et al.*, 2017; von Bredow *et al.*, 2021). For example, although von Bredow *et al.* (2021) described granules in the cytoplasm of specific cells, these were not identified as granulocytes; moreover, light microscopy analysis performed in that study did not allow identification of lamellocyte-like cells and adipohemocytes. Most importantly, our ultrastructural analysis was fundamental to unravel the morphofunctional modifications of

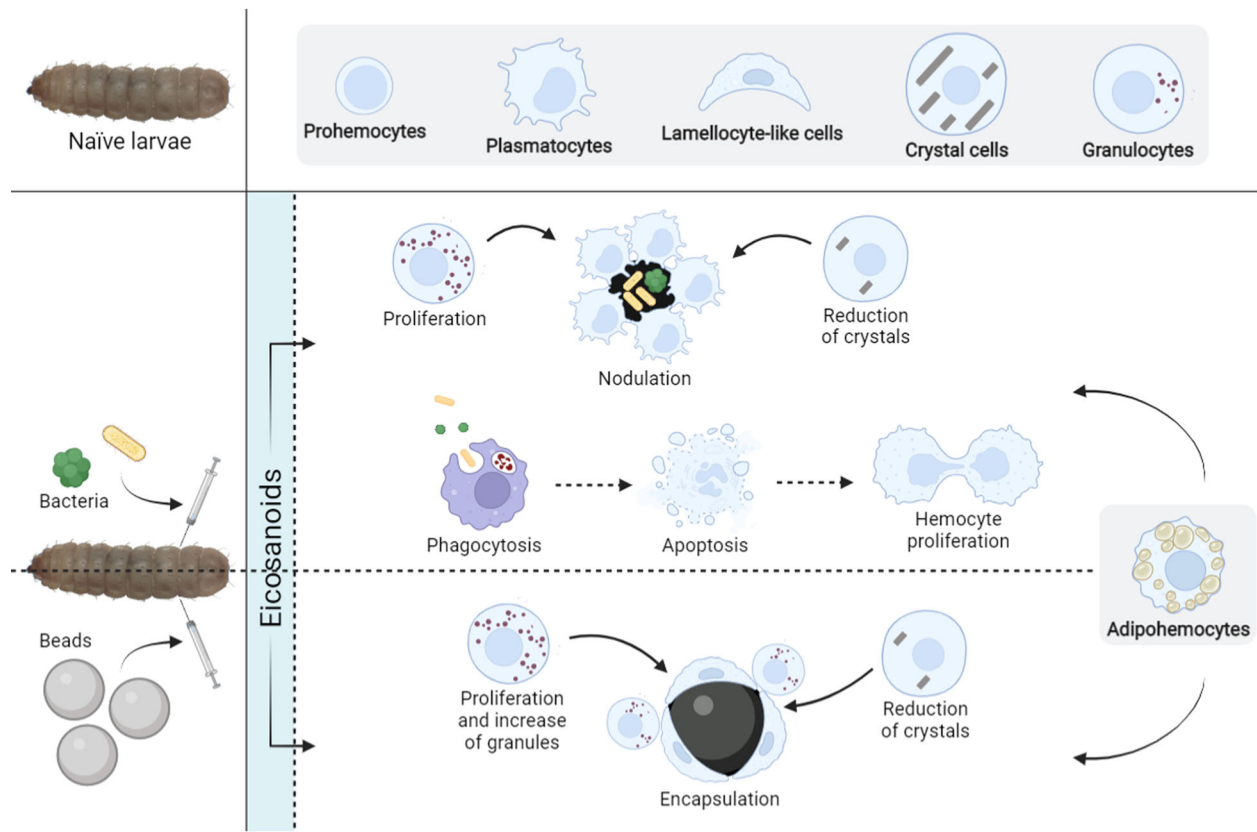


Fig. 10 Schematic representation of morphofunctional modifications of *Hermetia illucens* larval hemocytes in response to immune challenge. The different types of hemocytes are framed in gray.

hemocytes upon different immune challenges and the potential role of these cells. Although the use of specific cellular and molecular markers is mandatory to further characterize BSF hemocytes, this study, together with an in-depth knowledge of the humoral components (Bruno *et al.*, 2021) and of the role of the midgut as a protective organ against infections (Bonelli *et al.*, 2019; Bruno *et al.*, 2019b), will provide us with a better understanding of the physiological mechanisms that help BSF larvae to survive within rearing substrates that are extremely rich in microbes, which would be harmful for most insect species.

Acknowledgments

This work was supported by Fondazione Cariplo (grant number 2020-0900). We thank Sherryl Sundell for English editing. The authors appreciated the support from Consorzio Interuniversitario per le Biotecnologie (CIB).

Aurora Montali was supported by a postdoctoral fellowship funded by University of Insubria.

Open Access Funding provided by Università degli Studi dell'Insubria within the CRUI-CARE Agreement.

Disclosure

The authors declare no competing financial interests.

References

- Araújo, H.C.R., Cavalcanti, M.G.S., Santos, S.S., Alves, L.C. & Brayner F.A. (2008) Hemocytes ultrastructure of *Aedes aegypti* (Diptera: Culicidae). *Micron*, 39, 184–189.
- Belazi, D., Solé-Domènech, S., Johansson, B., Schalling, M. & Sjövall, P. (2009) Chemical analysis of osmium tetroxide staining in adipose tissue using imaging ToF-SIMS. *Histochemistry and Cell Biology*, 132, 105–115.
- Bidla, G., Dushay, M.S. & Theopold, U. (2007) Crystal cell rupture after injury in *Drosophila* requires the JNK pathway,

- small GTPases and the TNF homolog Eiger. *Journal of Cell Science*, 120, 1209–1215.
- Boguś, M.I., Ligeża-Żuber, M., Polańska, M.A., Mosiewicz, M., Włoka, E. & Sobocińska, M. (2018) Fungal infection causes changes in the number, morphology and spreading ability of *Galleria mellonella* haemocytes. *Physiological Entomology*, 43, 214–226.
- Bonelli, M., Bruno, D., Caccia, S., Sgambetterra, G., Cappellozza, S., Jucker, C., *et al.* (2019) Structural and functional characterization of *Hermetia illucens* larval midgut. *Frontiers in Physiology*, 10, 204.
- Brehélin, M. (1982) Comparative study of structure and function of blood cells from two *Drosophila* species. *Cell and Tissue Research*, 221, 607–615.
- Bruno, D., Bonelli, M., Cadamuro, A.G., Reguzzoni, M., Grimaldi, A., Casartelli, M., *et al.* (2019a) The digestive system of the adult *Hermetia illucens* (Diptera: Stratiomyidae): morphological features and functional properties. *Cell and Tissue Research*, 378, 221–238.
- Bruno, D., Bonelli, M., De Filippis, F., Di Lelio, I., Tettamanti, G., Casartelli, M., *et al.* (2019b) The intestinal microbiota of *Hermetia illucens* larvae is affected by diet and shows a diverse composition in the different midgut regions. *Applied and Environmental Microbiology*, 85, e01864–18.
- Bruno, D., Montali, A., Mastore, M., Brivio, M.F., Mohamed, A., Tian, L., *et al.* (2021) Insights into the immune response of the black soldier fly larvae to bacteria. *Frontiers in Immunology*, 12, 4866.
- Cappellozza, S., Leonardi, M.G., Savoldelli, S., Carminati, D., Rizzolo, A., Cortellino, G., *et al.* (2019) A first attempt to produce proteins from insects by means of a circular economy. *Animals*, 9, 278.
- Castillo, J.C., Robertson, A.E. & Strand, M.R. (2006) Characterization of hemocytes from the mosquitoes *Anopheles gambiae* and *Aedes aegypti*. *Insect Biochemistry and Molecular Biology*, 36, 891–903.
- Cho, Y. & Cho, S. (2019) Hemocyte-hemocyte adhesion by granulocytes is associated with cellular immunity in the cricket, *Gryllus bimaculatus*. *Scientific Reports*, 9, 18066.
- Corcoran, S. & Brückner, K. (2020) Quantification of blood cells in *Drosophila melanogaster* and other insects. *Immunity in Insects* (eds F. Sandrelli & G. Tettamanti), pp. 65–77. Humana, New York.
- Costa, S.C., Ribeiro, C., Girard, P.A., Zumbihl, R. & Brehélin, M. (2005) Modes of phagocytosis of Gram-positive and Gram-negative bacteria by *Spodoptera littoralis* granular haemocytes. *Journal of Insect Physiology*, 51, 39–46.
- Dean, P., Richards, E.H., Edwards, J.P., Reynolds, S.E. & Charnley, K. (2004) Microbial infection causes the appearance of hemocytes with extreme spreading ability in monolayers of the tobacco hornworm *Manduca sexta*. *Developmental & Comparative Immunology*, 28, 689–700.
- Dorrah, M.A., Mohamed, A.A. & Shaurub, E.H. (2019) Immunosuppressive effects of the limonoid azadirachtin, insights on a nongenotoxic stress botanical, in flesh flies. *Pesticide Biochemistry and Physiology*, 153, 55–66.
- Eleftherianos, I., Heryanto, C., Bassal, T., Zhang, W., Tettamanti, G. & Mohamed, A. (2021a) Haemocyte-mediated immunity in insects: cells, processes and associated components in the fight against pathogens and parasites. *Immunology*, 164, 401–432.
- Eleftherianos, I., Zhang, W., Heryanto, C., Mohamed, A., Contreras, G., Tettamanti, G., *et al.* (2021b) Diversity of insect antimicrobial peptides and proteins—a functional perspective: A review. *International Journal of Biological Macromolecules*, 191, 277–287.
- Faraldo, A.C. & Lello, E. (2003) Defense reactions of *Dermatobia hominis* (Diptera: Cuterebridae) larval hemocytes. *Bio-cell*, 27, 197–203.
- Franchini, A., Miyan, J.A. & Ottaviani, E. (1996) Induction of ACTH-and TNF- α -like molecules in the hemocytes of *Calliphora vomitoria* (Insecta, Diptera). *Tissue and Cell*, 28, 587–592.
- Gábor, E., Cinege, G., Csordás, G., Rusvai, M., Honti, V., Kolics, B., *et al.* (2020) Identification of reference markers for characterizing honey bee (*Apis mellifera*) hemocyte classes. *Development and Comparative Immunology*, 109, 103701.
- Giulianini, P.G., Bertolo, F., Battistella, S. & Amirante, G.A. (2003) Ultrastructure of the hemocytes of *Cetonischema aeruginosa* larvae (Coleoptera, Scarabaeidae): involvement of both granulocytes and oenocytoids in *in vivo* phagocytosis. *Tissue and Cell*, 35, 243–251.
- Gorman, M.J., Schwartz, A.M. & Paskewitz, S.M. (1998) The role of surface characteristics in eliciting humoral encapsulation of foreign bodies in *Plasmodium*-refractory and -susceptible strains of *Anopheles gambiae*. *Journal of Insect Physiology*, 44, 947–954.
- Hawkey, K.J., Lopez-Viso, C., Brameld, J.M., Parr, T. & Salter, A.M. (2021) Insects: a potential source of protein and other nutrients for feed and food. *Annual Review of Animal Biosciences*, 9, 333–354.
- Hillyer, J.F. & Christensen, B.M. (2002) Characterization of hemocytes from the yellow fever mosquito, *Aedes aegypti*. *Histochemistry and Cell Biology*, 117, 431–440.
- Hillyer, J.F., Schmidt, S.L. & Christensen, B.M. (2003a) Hemocyte-mediated phagocytosis and melanization in the mosquito *Armigeres subalbatus* following immune challenge by bacteria. *Cell and Tissue Research*, 313, 117–127.
- Hillyer, J.F., Schmidt, S.L. & Christensen, B.M. (2003b) Rapid phagocytosis and melanization of bacteria and *Plasmodium* sporozoites by hemocytes of the mosquito *Aedes aegypti*. *Journal of Parasitology*, 89, 62–69.

- Hogsette, J.A. (1992) New diets for production of house flies and stable flies (Diptera: Muscidae) in the laboratory. *Journal of Economic Entomology*, 85, 2291–2294.
- Hwang, S., Bang, K., Lee, J. & Cho, S. (2015) Circulating hemocytes from larvae of the Japanese rhinoceros beetle *Alomyrina dichotoma* (Linnaeus) (Coleoptera: Scarabaeidae) and the cellular immune response to microorganisms. *PLoS ONE*, 10, e0128519.
- Jung, S.H., Evans, C.J., Uemura, C. & Banerjee, U. (2005) The *Drosophila* lymph gland as a developmental model of hematopoiesis. *Development*, 132, 2521–2533.
- Jung, S., Jung, J.M., Tsang, Y.F., Bhatnagar, A., Chen, W.H., Lin, K.Y.A., et al. (2022) Biodiesel production from black soldier fly larvae derived from food waste by non-catalytic transesterification. *Energy*, 238, 121700.
- Kaaya, G.P. & Ratcliffe, N.A. (1982) Comparative study of hemocytes and associated cells of some medically important dipterans. *Journal of Morphology*, 173, 351–365.
- Kaaya, G.P., Ratcliffe, N.A. & Alemu, P. (1986) Cellular and humoral defenses of *Glossina* (Diptera: Glossinidae): reactions against bacteria, trypanosomes, and experimental implants. *Journal of Medical Entomology*, 1, 30–43.
- Kim, Y., Ahmed, S., Stanley, D. & An, C. (2018) Eicosanoid-mediated immunity in insects. *Developmental and Comparative Immunology*, 83, 130–143.
- Kim, Y., Ahmed, S., Al Baki, M.A., Kumar, S., Kim, K., Park, Y., et al. (2020) Deletion mutant of PGE₂ receptor using CRISPR-Cas9 exhibits larval immunosuppression and adult infertility in a lepidopteran insect, *Spodoptera exigua*. *Developmental and Comparative Immunology*, 111, 103743.
- Kwon, H., Bang, K. & Cho, S. (2014) Characterization of the hemocytes in larvae of *Protaetia brevitarsis seulensis*: involvement of granulocyte-mediated phagocytosis. *PLoS ONE*, 9, e103620.
- Lanot, R., Zachary, D., Holder, F. & Meister, M. (2001) Postembryonic hematopoiesis in *Drosophila*. *Developmental Biology*, 230, 243–257.
- Lavine, M.D. & Strand, M.R. (2002) Insect hemocytes and their role in immunity. *Insect Biochemistry and Molecular Biology*, 32, 1295–1309.
- Lemaitre, B. & Hoffmann, J. (2007) The host defense of *Drosophila melanogaster*. *Annual Review of Immunology*, 25, 697–743.
- Li, T., Yan, D., Wang, X., Zhang, L. & Chen, P. (2019) Hemocyte changes during immune melanization in *Bombyx mori* infected with *Escherichia coli*. *Insects*, 10, 301.
- Ling, E. & Yu, X. Q. (2006) Cellular encapsulation and melanization are enhanced by immunectins, pattern recognition receptors from the tobacco hornworm *Manduca sexta*. *Developmental & Comparative Immunology*, 30, 289–299.
- Manachini, B., Arizza, V., Parrinello, D. & Parrinello, N. (2011) Hemocytes of *Rhynchophorus ferrugineus* (Olivier) (Coleoptera: Curculionidae) and their response to *Saccharomyces cerevisiae* and *Bacillus thuringiensis*. *Journal of Invertebrate Pathology*, 106, 360–365.
- Mandato, G.A., Diehl-Jones, L., Moore, S.J. & Downer, R.G. (1997) The effect of eicosanoid biosynthesis inhibitors on prophenoloxidase activation, phagocytosis and cell spreading in *Galleria mellonella*. *Journal of Insect Physiology*, 43, 1–8.
- Meister, M. (2004) Blood cells of *Drosophila*: cell lineages and role in host defence. *Current Opinion in Immunology*, 16, 10–15.
- Meister, M. & Lagueux, M. (2003) *Drosophila* blood cells. *Cellular Microbiology*, 5, 573–580.
- Nakahara, Y., Shimura, S., Ueno, C., Kanamori, Y., Mita, K., Kiuchi, M., et al. (2009) Purification and characterization of silkworm hemocytes by flow cytometry. *Developmental and Comparative Immunology*, 33, 439–448.
- Nuvoli, D., Montevicchi, G., Lovato, F., Masino, F., Van Der Borgh, M., Messori, M., et al. (2021) Protein films from black soldier fly (*Hermetia illucens*, Diptera: Stratiomyidae) prepupae: effect of protein solubility and mild crosslinking. *Journal of the Science of Food and Agriculture*, 101, 4506–4513.
- Pal, R. & Kumar, K. (2014) A comparative study of haemocytes in three cyclorrhaphous dipteran flies. *International Journal of Tropical Insect Science*, 34, 207–216.
- Paro, S. & Imler, J.L. (2016) Immunity in insects. *Encyclopedia of Immunobiology, Volume 1* (eds M.J.H. Ratcliffe), pp. 454–461. Academic Press, New York.
- Pech, L.L. & Strand, M.R. (1996) Granular cells are required for encapsulation of foreign targets by insect haemocytes. *Journal of Cell Science*, 109, 2053–2060.
- Pimentel, A.C., Montali, A., Bruno, D. & Tettamanti, G. (2017) Metabolic adjustment of the larval fat body in *Hermetia illucens* to dietary conditions. *Journal of Asia-Pacific Entomology*, 20, 1307–1313.
- Ribeiro, C. & Brehélin, M. (2006) Insect haemocytes: what type of cell is that? *Journal of Insect Physiology*, 52, 417–429.
- Riccardi, C. & Nicoletti, I. (2006) Analysis of apoptosis by propidium iodide staining and flow cytometry. *Nature Protocols*, 1, 1458–1461.
- Rizki, T.M. & Rizki, R.M. (1992) Lamellocyte differentiation in *Drosophila* larvae parasitized by *Leptopilina*. *Developmental & Comparative Immunology*, 16, 103–110.
- Roy, M.C. & Kim, Y. (2021) Eicosanoid-induced calcium signaling mediates cellular immune responses of *Tenebrio molitor*. *Entomologia Experimentalis et Applicata*, 169, 888–898.
- Salama, H.S. & Sharaby, A. (1985) Histopathological changes in *Heliothis armigera* infected with *Bacillus thuringiensis* as detected by electron microscopy. *International Journal of Tropical Insect Science*, 6, 503–511.

- Satyavathi, V.V., Minz, A. & Nagaraju, J. (2014) Nodulation: an unexplored cellular defense mechanism in insects. *Cellular Signalling*, 26, 1753–1763.
- Schmit, A.R., Rowley, A.F. & Ratcliffe, N.A. (1977) The role of *Galleria mellonella* hemocytes in melanin formation. *Journal of Invertebrate Pathology*, 29, 232–234.
- Schmitz, A., Anselme, C., Ravallec, M., Rebuf, C., Simon, J.C., Gatti, J.L., *et al.* (2012) The cellular immune response of the pea aphid to foreign intrusion and symbiotic challenge. *PLoS ONE*, 7, e42114.
- Shrestha, S., Stanley, D. & Kim, Y. (2011) PGE₂ induces oenocytoid cell lysis via a G protein-coupled receptor in the beet armyworm, *Spodoptera exigua*. *Journal of Insect Physiology*, 57, 1568–1576.
- Silva, J.E.B., Boleli, I.C. & Simões, Z.L.P. (2002) Hemocyte types and total and differential counts in unparasitized and parasitized *Anastrepha obliqua* (Diptera, Tephritidae) larvae. *Brazilian Journal of Biology*, 62, 689–699.
- Smith, R.C., King, J.G., Tao, D., Zeleznik, O.A., Brando, C., Thallinger, G.G., *et al.* (2016) Molecular profiling of phagocytic immune cells in *Anopheles gambiae* reveals integral roles for hemocytes in mosquito innate immunity. *Molecular & Cellular Proteomics*, 15, 3373–3387.
- Sorrentino, R.P., Carton, Y. & Govind, S. (2002) Cellular immune response to parasite infection in the *Drosophila* lymph gland is developmentally regulated. *Developmental Biology*, 243, 65–80.
- Stanley, D. (2006) Prostaglandins and other eicosanoids in insects: biological significance. *Annual Review of Entomology*, 51, 25–44.
- Stanley, D. & Kim, Y. (2014) Eicosanoid signaling in insects: from discovery to plant protection. *Critical Reviews in Plant Sciences*, 33, 20–63.
- Strand, M.R. (2008) The insect cellular immune response. *Insect Science*, 15, 1–14.
- Tan, J., Xu, M., Zhang, K., Wang, X., Chen, S., Li, T., *et al.* (2013) Characterization of hemocytes proliferation in larval silkworm, *Bombyx mori*. *Journal of Insect Physiology*, 59, 595–603.
- Tettamanti, G., Van Campenhout, L. & Casartelli, M. (2022) A hungry need of knowledge on the black soldier fly larvae. *Journal of Insects as Food and Feed*, 8, 217–222.
- Tojo, S., Naganuma, F., Arakawa, K. & Yokoo, S. (2000) Involvement of both granular cells and plasmatocytes in phagocytic reactions in the greater wax moth, *Galleria mellonella*. *Journal of Insect Physiology*, 46, 1129–1135.
- Vogel, H., Müller, A., Heckel, D.G., Gutzeit, H. & Vilcinskas, A. (2018) Nutritional immunology: diversification and diet-dependent expression of antimicrobial peptides in the black soldier fly *Hermetia illucens*. *Developmental & Comparative Immunology*, 78, 141–148.
- Vogel, M., Shah, P.N., Voulgari-Kokota, A., Maistrou, S., Aartsma, Y., Beukeboom, L.W., *et al.* (2022) Health of the black soldier fly and house fly under mass-rearing conditions: innate immunity and the role of the microbiome. *Journal of Insects as Food and Feed*, 8, 857–878.
- von Bredow, Y.M., Müller, A., Popp, P.F., Iliasov, D. & von Bredow, C.R. (2021) Characterisation and mode of action analysis of black soldier fly (*Hermetia illucens*) larva derived haemocytes. *Insect Science*, 29, 1071–1095.
- Wrońska, A.K., Kaczmarek, A., Kazek, M. & Boguś, M.I. (2022) Infection of *Galleria mellonella* (Lepidoptera) larvae with the entomopathogenic fungus *Conidiobolus coronatus* (Entomophthorales) induces apoptosis of hemocytes and affects the concentration of eicosanoids in the hemolymph. *Frontiers in Physiology*, 12, 774086.
- Wu, G., Li, M., Liu, Y., Ding, Y. & Yi, Y. (2015) The specificity of immune priming in silkworm, *Bombyx mori*, is mediated by the phagocytic ability of granular cells. *Journal of Insect Physiology*, 81, 60–68.
- Zdybicka-Barabas, A., Bulak, P., Polakowski, C., Bieganowski, A., Waśko, A. & Cytryńska, M. (2017) Immune response in the larvae of the black soldier fly *Hermetia illucens*. *Invertebrate Survival Journal*, 14, 9–17.

Manuscript received June 1, 2022

Final version received August 3, 2022

Accepted August 18, 2022

Supporting Information

Additional supporting information may be found online in the Supporting Information section at the end of the article.

Fig. S1 Effects of needle puncture and PBS injection on the hemocyte response of black soldier fly larvae.

Fig. S2 H3P immunocytochemistry.